

*Note: this non-peer reviewed preprint. It has been submitted to a peer-reviewed journal for publication.*

## **Wildfire influence on recent US pollution trends**

December 15, 2022

Marshall Burke<sup>1,2,3,\*</sup>, Marissa L. Childs<sup>4,\*</sup>, Brandon de la Cuesta<sup>2</sup>, Minghao Qiu<sup>5</sup>, Jessica Li<sup>2</sup>, Carlos F. Gould<sup>5</sup>, Sam Heft-Neal<sup>2</sup>, Michael Wara<sup>1,6</sup>

<sup>1</sup>Doerr School of Sustainability, Stanford University

<sup>2</sup>Center on Food Security and the Environment, Stanford University

<sup>3</sup>National Bureau of Economic Research

<sup>4</sup>Center for the Environment, Harvard University

<sup>5</sup>Department of Earth System Science, Stanford University

<sup>6</sup>Woods Institute of the Environment, Stanford University

\*These authors contributed equally to the manuscript.

### ABSTRACT

**Steady improvements in ambient air quality in the US over the past several decades have led to large public health benefits. However, recent trends in PM<sub>2.5</sub> concentrations, a key pollutant, have stagnated or begun to reverse throughout much of the US. We quantify the contribution of wildfire smoke to these trends and find that since 2016, wildfire smoke has significantly slowed or reversed previous improvements in average annual PM<sub>2.5</sub> concentrations in two-thirds of US states, eroding 23% of previous gains on average in those states (equivalent to 3.6 years of air quality progress) and over 50% in multiple western states. Smoke influence on trends in extreme PM<sub>2.5</sub> concentrations is detectable by 2010, but remains concentrated primarily in western states. Wildfire-driven increases in ambient PM<sub>2.5</sub> concentrations are unregulated under current air pollution law, and, absent additional intervention, wildfire's contribution to regional and national air quality trends is likely to grow as the climate continues to warm.**

The observed multi-decadal decline in key ambient air pollutant concentrations across the US has been widely celebrated, both for its demonstrated human health benefits and because it was substantially a result of bipartisan public policy choices, in particular the Clean Air Act and its amendments (1). Recent data, however, suggest that these air quality gains are stagnating or even reversing across nearly all of the US (Fig 1), raising questions about whether past progress is being durably undone, what is causing the undoing, and if or how policy should respond.

Here we study the contribution of growing wildfire activity to recent trends in ambient PM<sub>2.5</sub> concentrations. Wildfires have increased in size and severity in recent years, a consequence of a

century of fire suppression in western forests that have left abundant fuels on the ground and a warming climate that has made these fuels more arid and flammable (2, 3). Increased fire activity has in turn led to increases in the emission and formulation of key air pollutants, including “criteria” pollutants such as particulate matter with diameters less than 2.5 microns ( $PM_{2.5}$ ). These pollutants are regulated in the US under the Clean Air Act and have been shown to have a wide array of negative health impacts (4). Studies using data prior to 2016 concluded that the wildfire contribution to measured  $PM_{2.5}$  concentrations was apparent mainly in the northwest of the contiguous US (CONUS), but disagreed over whether enhancements in this region were observable in average annual concentrations or only in extreme daily concentrations (5, 6). Studies that include more recent data from the very active 2018 and 2020 wildfire seasons conclude that the imprint of wildfire smoke on surface average and extreme  $PM_{2.5}$  concentrations has expanded substantially in geographic scope, with observed enhancements throughout much of the Western US (7, 8). Research also suggests that wildfire smoke is increasingly implicated in “exceptional event” designations, or days on which regulators exempt observed pollutant concentrations from determination of regulatory attainment under the Clean Air Act because the source of the pollution was deemed beyond control of local authorities (9).

Yet wildfires are clearly not the only possible contributor to recent air quality trends. A large body of work shows how changes in methods of production in the energy, manufacturing, and other industrial sectors, changes in agricultural production practices, and changes in global trade patterns have shaped short- and long-term variation in air pollution concentrations throughout the US (10–12). Accurate and up-to-date characterization of the drivers of recent air quality trends is important to informing policy decisions about how to regulate or improve air quality, and whether interventions should be targeted to specific regions.

To isolate the contribution of wildfire smoke to pollution concentrations, we build on earlier work (6, 8) and use a combination of ground- and satellite-based measurements to isolate the component of surface  $PM_{2.5}$  concentrations attributable to wildfire smoke. Specifically, our primary analysis combines daily data from thousands of regulatory pollution monitoring stations from across the US with satellite- and analyst-based estimates of when and where wildfire smoke is in the air (Fig S1). Using data from 2006-2022, we calculate daily  $PM_{2.5}$  anomalies from season- and time period-specific median concentrations at each location and attribute these anomalies to wildfire if satellite images indicate a wildfire plume is overhead on a given day (Methods). For this approach to successfully isolate wildfire’s contribution to surface  $PM_{2.5}$ , it must be the case that satellite-derived plume estimates accurately describe the location of wildfire smoke, and that the presence or absence of a plume is not systematically correlated with other non-wildfire sources of variation in surface  $PM_{2.5}$ . Using measurement data on the chemical components

of  $PM_{2.5}$  and panel regression, ref (8) shows that both these conditions are likely to hold. See Methods for a discussion of the advantages of this ground station-based approach relative to alternatives. Non-wildfire  $PM_{2.5}$  on a given day can then be calculated as the difference between total observed and wildfire-attributed  $PM_{2.5}$ . Total, wildfire, or non-wildfire  $PM_{2.5}$  can be spatially or temporally aggregated to characterize wildfire's contribution to average or extreme daily  $PM_{2.5}$  concentrations. We focus on two measures of ambient air quality: annual average  $PM_{2.5}$  concentrations, calculated as the simple average of daily  $PM_{2.5}$  concentrations at a given station in a year, and the proportion of days above  $35\mu g/m^3$  at each station over a year, a concentration threshold currently used as part of Clean Air Act attainment designations.

To characterize trends in total or non-smoke  $PM_{2.5}$  averages and extremes and to test whether trends in each have changed over time, we divide our sample into “early” and “recent” periods, estimate trends in pollutant concentrations in each period, and then test whether trends are statistically different ( $p < 0.05$ ) between the two periods. To inform period definitions, we conduct formal tests for trend breaks (13) on data pooled across all stations in CONUS and then separately in each US climate region (Methods). CONUS-wide data indicate a trend break in 2016 for annual average  $PM_{2.5}$ , and in 2010 for extreme daily  $PM_{2.5}$ , consistent with visual evidence (Fig S2). Region-specific tests identify trend breaks for average  $PM_{2.5}$  within a few years of 2016 in most states, but suggest that breaks might have been earlier in some western states (Fig S3). Region-specific tests for breaks in extreme daily  $PM_{2.5}$  concentrations also suggest regional breaks similar to CONUS-wide averages (Fig S4). Trend breaks in extreme days in the eastern US occurred at least in part because, remarkably, most states nearly eliminated the occurrence of such days around year 2010, despite averaging 10 of these days per year from 2000 - 2002.

Based on these results, our main analysis defines early and recent periods in a common way across CONUS, with the early period beginning in 2000 when systematic monitoring of  $PM_{2.5}$  began, and the recent period beginning in 2016 for annual average  $PM_{2.5}$  and in 2010 for extreme daily  $PM_{2.5}$ ; data for the recent period include data through October 2022 (Methods). To test whether trends in average or extreme  $PM_{2.5}$  are different between periods, we fit linear panel regressions to all stations in each geographic region of interest in each period, allowing average pollution levels to differ across stations but estimating a common trend across stations within each region for each period (Methods). We then test whether total  $PM_{2.5}$  trends are statistically different in the two periods in each region to identify “stagnations”, or states where declines in total  $PM_{2.5}$  slowed in the recent period, or “reversals”, states in which  $PM_{2.5}$  was declining in the early period but increasing in the recent period. Finally, using our measure of smoke  $PM_{2.5}$ , we identify “smoke-influenced” regions as those where post-period trends in total  $PM_{2.5}$  were statistically distinguishable from trends in non-smoke  $PM_{2.5}$  (Methods; Table S1). Our breakpoint analysis

and descriptive analysis focus on US climate regions, consistent with the public trend data published by EPA (14) that relies on a smaller set of long-reporting stations. To characterize smoke influence, our main analysis uses a larger sample of stations and focuses on smaller geographies (states), in part because states have jurisdictional responsibility under the Clean Air Act.

We test robustness to alternate period breaks, to exclusion of recent extreme wildfire years, and to alternate statistical approaches to estimating pollution trends on either side of the break. Because individual stations come online at different times and report at different daily frequencies, we also test robustness to sample restrictions that limit stations to those reporting more frequently and/or reporting for more years in the sample (Methods). Finally, we note that trends in a state or region's  $PM_{2.5}$  concentrations need not necessarily reflect trends in that region's emissions of particulates and their precursors, given that wildfire smoke often travels long distances (15).

## Results

In 42 out of 48 states in CONUS, average annual  $PM_{2.5}$  concentrations were declining over the period 2000-2016 but then either significantly slowed (25 “stagnating” states) or began to reverse (17 “reversing” states) (Fig 2a). In the remaining 6 states, either early trends were not declining or trends in annual average  $PM_{2.5}$  were not statistically different between early and recent periods.

We find that wildfire smoke statistically significantly influenced recent trends in annual average total  $PM_{2.5}$  in 31 of these 42 stagnating or reversing states – representing 65% of all CONUS states. In 18 of these 31 states,  $PM_{2.5}$  was still declining or flat in the recent period but would have declined faster absent smoke. These states are located throughout much of the US Midwest, South, and East (Fig 3). We calculate that from 2016 to 2022, smoke added  $0.9\mu g/m^3$  to annual  $PM_{2.5}$  concentrations in these 18 states (median), equivalent to 13% of the  $PM_{2.5}$  declines achieved in these states between 2000-2016, or 2.1 years of median progress during those years (Fig 2b,c).

In 13 other states, total  $PM_{2.5}$  was trending significantly up since 2016, but would have either trended up more slowly (8 states) or would have actually trended down (5 states) absent smoke. These states are concentrated in the US West and Midwest, and we calculate that smoke added  $1.1\mu g/m^3$  to  $PM_{2.5}$  concentrations in these states since 2016, equivalent to 40% of the average decline in annual  $PM_{2.5}$  achieved in these states between 2000-2016, or 6.3 years of progress during those years.

The remainder of states either had no detectable smoke influence in the recent period, such as many states in the Northeast or, in the case of Idaho and Nevada, were smoke influenced in the recent period but did not have  $PM_{2.5}$  trending down in the early period. A small number of northern Rockies states, including Montana and Wyoming, had heavy smoke exposures in recent years, but the small number of monitoring stations and high year-to-year variance in pollution in those states meant that we could not detect a statistically significant influence of wildfires on recent trends. We emphasize that our measure of “influence” is in regard to pollution trends rather than pollution levels, and that most western states have had substantial amplification of pollution levels due to wildfire smoke in certain recent years (8), even if influence on trends is sometimes less apparent.

State-level estimates of pollution trends and their categorization regarding stagnating/reversing and smoke influence are largely robust to alternate estimation samples and approaches, including limiting the sample of stations to those reporting in most years and utilizing region-specific sample breakpoints for trend estimation (Figs S5 and S6 for trend estimates, Tables S2 and S3 and Figs S7 and S8 for categorizations). Results are most sensitive to whether one fits separate models on either side of the breakpoint (our main model) or estimates a single piecewise regression with a change in slope at the breakpoint; piecewise trend estimates suggest that 14 of 48 states experienced smoke-influenced changes in  $PM_{2.5}$  trends. Estimates are also somewhat sensitive to dropping observations from 2021, which was the most smoke-influenced year in our sample; without 2021 in the sample, we estimate that 19 out of 48 states are “smoke-influenced” (Table S3). Notably, we find largely similar results when using break years prior to 2016 for states in the West, where region-specific breakpoint analysis suggests total  $PM_{2.5}$  trends were changing as early as 2010 (Fig S9). Results are robust to several different station inclusion criteria and additional modeling strategies (Methods, Figs S5 - S8 and Tables S2 - S3).

**Wildfire influence on daily  $PM_{2.5}$  extremes** By 2010, most states in the central, eastern, and southern US saw the near-elimination of days on which  $PM_{2.5}$  concentrations exceeded  $35\mu g/m^3$  (Fig S10). Thus there was an observed trend break in extreme smoke  $PM_{2.5}$  in these states (Fig S4), but these breaks were driven by states hitting zero extreme pollution days, thus eliminating the opportunity for further declines. By contrast, most states in the western US have seen consistent, if variable, increases in the number of extreme days since 2010.

We find substantial smoke influence on trends in extreme  $PM_{2.5}$  days in western States. In 13 states, we find clear evidence that, since 2010, the observed increase in days above  $35\mu g/m^3$  would have been smaller without smoke (Fig S10). In the remaining 35 states, we did not de-

test an influence of smoke on recent trends in daily extremes. These counts are robust to alternate samples, break years, and estimation approaches (Fig S11, Table S4).

We then calculate the proportion of days where wildfire smoke was the cause of the threshold exceedance – i.e., days in which the  $35\mu\text{g}/\text{m}^3$  threshold would not have been exceeded absent wildfire smoke on that day – using the sample of EPA stations with at least 15 years of data with over 50 observations per year during 2000 - 2022. As station intermittency could still impact estimates by overweighting certain years, we first calculate state-year averages and then average these to get state average over a specified time period. From 2006 to 2010, in no states did wildfire smoke cause more than 25% of daily  $35\mu\text{g}/\text{m}^3$  exceedances (Fig S12). Between 2011 and 2022, wildfire smoke caused at least 25% of exceedances in 7 states (Washington, Oregon, Montana, Idaho, Nevada, North Dakota, and South Dakota). In the the last 3 years of the sample (2020-2022), wildfire smoke caused at least 25% of daily exceedances in 21 states, and caused more than 75% of exceedances in 4 states (Washington, Oregon, Montana, and Idaho). We conclude that wildfire smoke has been a substantial cause of increases in daily  $\text{PM}_{2.5}$  extremes throughout most of the West, and that the influence of smoke on extremes now extends beyond the influence uncovered in previous analyses (5), which discerned influence only in the Pacific Northwest.

**Historical and future climatic influence** The recent rapid uptick in wildfire activity and resulting upward pressure on annual and extreme  $\text{PM}_{2.5}$  concentrations throughout the western US raises the question of whether recent  $\text{PM}_{2.5}$  trends are likely to continue or whether they were driven by idiosyncratic variability in climatic conditions that are unlikely to persist. Many studies have sought to understand climatic drivers of recent increases in fire activity and to project future changes in these drivers. Together, these studies provide strong evidence that interannual variation in climate-related factors such as fuel aridity and fire weather are a primary driver of recent variation in fire activity, and that projected future changes in these variables from global climate models indicate that – absent intervention – fire activity is likely to further increase as the climate warms (2, 16), although the magnitude of that increase is somewhat sensitive to the climate variable used to project changes in wildfire activity (17). Using a variety of modeling approaches, studies also relate projected increases in wildfire activity to potential changes in surface air quality over the next century, finding large possible increases in average and daily extreme  $\text{PM}_{2.5}$  concentrations (18, 19).

To further corroborate these results, we calculate annual summertime (May-Sept) average vapor pressure deficit (VPD) over western US forests, and relate these values to our measures of annual average smoke  $\text{PM}_{2.5}$ , using all available monitoring stations across the Western US (defined

here as all states west of, and including, New Mexico, Colorado, Wyoming, and Montana). VPD is strongly related to the log of smoke  $\text{PM}_{2.5}$  (Fig 4a), explaining roughly half of the interannual variation in western smoke since 2006. The estimated relationship is robust to first detrending both VPD and smoke, and so is not spuriously driven by common time trends in both time series. VPD values have increased over western forests since 1980, and were at or near record maxima in 2020-2021 (Fig 4b).

Using an ensemble of 34 debiased global climate model projections (Methods), we find that projected *average* VPD levels over western forests by mid-century match or exceed recent historical extremes, even under low emissions scenarios (Fig 4b). Relative to observed VPD in the last three years of our sample (2020-2022), projected average increases in VPD under SSP3-7.0 imply an additional increase in annual average smoke  $\text{PM}_{2.5}$  concentrations of  $3.3\mu\text{g}/\text{m}^3$  by 2050, based on the log-linear relationship in (Fig 4a). This projected increase represents an annual growth rate in smoke  $\text{PM}_{2.5}$  in future years ( $0.12\mu\text{g}/\text{m}^3 \text{ yr}^{-1}$ ) that is roughly 60% of the annual growth rate observed during the 2016-2022 period in these western states ( $0.19\mu\text{g}/\text{m}^3 \text{ yr}^{-1}$ ). While more detailed, spatially-explicit modeling will help improve these estimates, they suggest that absent additional intervention (such as widespread fuels management in affected forests), recent trends in smoke  $\text{PM}_{2.5}$  will likely continue under a warming climate.

## Discussion

Approaches to air quality regulation have historically been built on two primary facts: most pollutant concentrations were the results of emissions tied directly to controllable human activity, and the sources of these emissions tended to be locally or regionally proximate to the population that they impact. Regulation based largely on these facts, such as the Clean Air Act, have contributed substantially to the remarkable decadal improvements in air quality averages and extremes observed throughout the US through the early 2010s (1) (Fig 1, Fig S2). These facts have also led to calls for location-specific approaches to reducing remaining pollution burdens and eliminating remaining disparities in exposures across socioeconomic groups (20). At present, EPA is currently in the process of reviewing and revising the level of permitted ambient  $\text{PM}_{2.5}$  under the Clean Air Act, based on updated scientific recommendations of 8-10  $\mu\text{g}/\text{m}^3$  annual average  $\text{PM}_{2.5}$  (21).

We show that recent increases in wildfire smoke have substantially slowed or reversed improvements in ambient  $\text{PM}_{2.5}$  concentrations throughout much of the US, with widespread recent in-

fluence on annual average PM<sub>2.5</sub> concentrations and regional influence on daily PM<sub>2.5</sub> extremes. These increases in wildfire smoke, which we and others show are expected to continue under a warming climate, subvert the logic of traditional, regionally-based air quality regulation focused on control of anthropogenic emission sources and could undermine location-specific approaches to reducing pollution burdens. This is because with wildfires, the emissions source is often not under the control of the impacted jurisdiction: increased surface pollutant concentrations in one location can originate from fires that are hundreds or thousands of kilometers away (15), and these fires have a more indirect – albeit quite substantial – link to human activity. While more recent US rule-making, such as the Cross-State Air Pollution Rule, recognizes that criteria pollutants often cross state boundaries, such regulation currently only pertains to large power plants in 27 states in the Eastern US. Further, wildfire smoke remains explicitly exempted from both local and transboundary attainment rules under the Clean Air Act, while at the same time, proposed approaches to better managing wildfire and wildfire smoke, via greater use of prescribed fire, are subject to regulation under the Act because they are considered anthropogenic emissions sources (22, 23). The growing influence of wildfire smoke on ambient PM<sub>2.5</sub> trends that we document suggests that a continuation of this current regulatory approach could increasingly fail to protect public health from poor ambient air quality.

New approaches will likely be needed to address the growing influence of wildfire smoke on air quality. These could include large-scale investment in fuels management to reduce extreme wildfire risk, as recently proposed by the US Forest Service (22); revision to key air quality regulation such that air quality exemptions during smoke days are only granted if efforts have been made to reduce wildfire risk; a default stance (or “rebuttable presumption”) that prescribed fire smoke emissions are exempt from regulation under the Clean Air Act, especially if annual average regulatory PM<sub>2.5</sub> standards are lowered; expansion of the geographic scope of regulatory implementation plans to include both source and impacted jurisdictions; and/or a shift in focus of air pollution programs towards exposure rather than emission reduction, implying large investment in indoor filtration to protect individuals and communities from the wildfire smoke events that increasingly occur (3, 9, 24). Given the complexity of wildfire smoke management, all of these measures may be required to avoid significant negative impacts on public health. Absent these or other interventions, wildfires’ contribution to poor air quality and adverse health impacts will likely continue to grow as the climate continues to warm.



## Methods

**Isolating wildfire smoke  $PM_{2.5}$**  We measure total  $PM_{2.5}$  at the daily level using data from 2,489 EPA air quality monitoring stations located throughout the contiguous US, where station-day average  $PM_{2.5}$  is calculated over all observations from monitors at a station location (Fig S1) (14, 25). To understand when smoke from fires may be affecting ground pollution levels, we follow earlier work (6, 8, 26) and construct a binary classification of smoke days for each station-day using data on smoke plumes from the National Oceanic and Atmospheric Administration (NOAA) Hazard Mapping System (HMS) (27), which are analyst-identified plume boundaries based on visible bands of satellite imagery (28–30). A station-day is classified as a smoke day if it falls within a smoke plume on a given day. The first full year for which the HMS plume data are available is 2006, which limits the start date of our smoke estimates.

We then combine ground station measurements with this classification of smoke days to define daily time series of smoke  $PM_{2.5}$  at each station. We first define  $PM_{2.5}$  anomalies as deviations from recent month- and location-specific median values on non-smoke days

$$\widetilde{PM}_{idmy} = PM_{idmy} - \overline{PM}_{imy}^{NS}, \quad (1)$$

where  $PM_{idmy}$  is the  $PM_{2.5}$  at station  $i$  on day  $d$  in month  $m$  and year  $y$  and  $\overline{PM}_{imy}^{NS}$  is the 3-year location- and month-specific median  $PM_{2.5}$  on non-smoke days. This median is calculated as

$$\overline{PM}_{IMY}^{NS} = \text{median}(\{PM_{idmy} | i = I, m = M, Y - 1 \leq y \leq Y + 1, \text{smoke}_{idmy} = 0\}), \quad (2)$$

with  $\text{smoke}_{idmy}$  a binary variable indicating smoke day classification, or when smoke may be affecting air pollution levels. We use medians rather than means to prevent days with extreme  $PM_{2.5}$  that are not smoke days from affecting the background  $PM_{2.5}$  estimates, as is occasionally the case in our data. Further, by using 3-year medians, we allow the measure of background non-smoke  $PM_{2.5}$  to evolve over time in each location to capture trends in non-smoke  $PM_{2.5}$  over time, including the many other changes sources of anthropogenic emissions. We then define smoke  $PM_{2.5}$  on each station-day as the anomaly above the median if there was a plume overhead, and zero otherwise:

$$\text{smoke}PM_{idmy} = \max(\widetilde{PM}_{idmy} * \text{smoke}_{idmy}, 0). \quad (3)$$

Our approach to isolating smoke  $PM_{2.5}$  at monitoring stations is similar to other recent work (6, 8, 26), and for it to successfully isolate wildfire’s contribution to surface  $PM_{2.5}$ , it must be the case that the HMS plumes accurately describe the location of wildfire smoke on a given day,

and that the presence or absence of a plume is not correlated with other non-wildfire sources of variation in surface  $PM_{2.5}$ . To the first concern, we find in our data that having a smoke plume overhead is associated with an average  $4.74 \mu\text{g}/\text{m}^3$  increase in  $PM_{2.5}$  after controlling for station-specific averages and average differences in  $PM_{2.5}$  between states, months, and years using fixed effects regression. We also find that in time series for specific stations, plumes align temporally with spikes in ground-measured  $PM_{2.5}$  (Fig. S1). We note that our approach does not require that plume heights or plume density be accurately measured by the satellite data; rather, we only need the plume data to tell us if there is any smoke in the atmospheric column, and then the magnitude of the ground-measured  $PM_{2.5}$  anomaly under the plume will tell us whether this smoke is mixing to the surface and how much it is affecting surface pollutant concentrations.

To the second concern about correlated time-varying non-smoke  $PM_{2.5}$  sources, Childs et al. (8) analyzed whether this method of constructing smoke  $PM_{2.5}$  from ground station anomalies is indeed picking up  $PM_{2.5}$  from smoke and not from other local time-varying sources of  $PM_{2.5}$  unrelated to smoke, using speciated data from Interagency Monitoring of Protected Visual Environments (IMPROVE) and Chemical Speciation Network (CSN) monitors. The authors found that species most likely to be present in smoke  $PM_{2.5}$  – in particular organic carbon – rose on smoke days but other non-fire-associated species (e.g., elemental carbon) did not rise. These results provide supporting evidence that our approach to isolating smoke  $PM_{2.5}$  from non-smoke  $PM_{2.5}$  is indeed picking up wildfire-sourced  $PM_{2.5}$  and not some other correlated  $PM_{2.5}$  source. Nevertheless, our measure of smoke days may still be a conservative estimate of the locations with air quality impacted by smoke: there likely remain undetected plumes under cloud cover, during nighttime periods when satellite-based plume segmentations are unavailable, or on days in which smoke is diffuse and difficult to identify in satellite imagery (6, 15). This will cause us to under-attribute  $PM_{2.5}$  to smoke and thus understate the influence of wildfire smoke on total  $PM_{2.5}$ .

Our main analysis uses data from 2000-2022. Because only data through October 21, 2022 were available at the time of analysis, we imputed the remainder of total  $PM_{2.5}$  and non-smoke  $PM_{2.5}$  for 2022 as the average value over October 22 through December 31 from the three previous three years. We will recompute the 2022 estimates with the full year of data once 2022 has ended and re-estimate all results; however, we do not expect our inferences to change as no large wildfires occurred between late October 2022 and December 2022. Data in Fig 1 are from the EPA's official public analysis of regional trends for each US climate region (31), using a subset of monitoring stations that report in every year; available data from this EPA analysis go through 2021.

Because we use data from fixed pollution stations to measure overall  $PM_{2.5}$  trends and wildfire

influence on them, our data will be representative of locations where stations are located. As stations are purposefully located in populated areas to assess Clean Air Act attainment, our estimates should be largely representative of CONUS populations. However, they will be less accurate for many rural areas in the Western US where stations are less common but where other estimates suggest wildfire influence on  $\text{PM}_{2.5}$  is often the strongest (8). Our implicitly population-weighted estimates thus likely understate the influence of smoke on total  $\text{PM}_{2.5}$  trends relative to an area-weighted estimate, and could understate wildfire influence in the rural West.

Finally, our approach to estimating trends in total, smoke, and non-smoke  $\text{PM}_{2.5}$  that combines satellites and ground stations is a complement to other potential approaches to measuring the influence of smoke on air quality trends, including approaches that rely on statistical analysis of station data alone (5) or that use emissions inventories and chemical transport models (6, 7). An advantage of our approach relative to solely station-based approaches is that satellite-derived plume data provide substantial information on the location of wildfire smoke plumes, and this information helps isolate the influence of wildfires from other time-trending sources of pollution exposure. An advantage of our approach relative to transport-based approaches is that it does not depend on uncertain wildfire emissions inventories, which have been shown to have large influence on predicted pollutant concentrations (32). Machine-learning based approaches for total and wildfire  $\text{PM}_{2.5}$ , and the gridded products they generate, provide an alternate approach (8, 33, 34), yet these products are generally estimated with some time lag and do not yet provide estimates for the most recent, heavy wildfire smoke years.

**Estimating breakpoints in  $\text{PM}_{2.5}$  trends** To guide our choice of how to divide our sample into early and recent periods for analysis, we follow ref (13) and implement an algorithmic approach to estimating break points in time series data. Under this approach, a breakpoint initialization value is chosen (the median time point by default) and the algorithm searches until the difference in slopes between its current and previous iteration is within a pre-specified tolerance level. Formally, in the single-breakpoint case the Muggeo algorithm fits the following iterative regression:

$$y_i = \beta_1 z_i + \beta_2 (z_i - \tilde{\psi})_+ + \gamma \mathbb{1}\{z_i > \tilde{\psi}\}^- \quad (4)$$

Where  $z_i$  is a numeric variable indexing time,  $\tilde{\psi}$  is the breakpoint value and is updated iteratively, and  $\hat{\gamma}$  measures the gap at a given iteration of breakpoint  $\hat{\psi}$  between the two fitted lines on either side of the breakpoint. The breakpoint is then updated between iterations, with  $\hat{\psi} = \tilde{\psi} + \frac{\hat{\gamma}}{\beta_2}$ . As the algorithm converges,  $\hat{\gamma}$  converges to zero and the algorithm ceases once it falls within a

pre-specified tolerance window. We set  $k = 1$  and search for the breakpoint at which  $\hat{\psi}$  falls below the default tolerance of  $10^{-5}$  suggested by Muggeo (35). We also constrain the algorithm to search only between the 20th and 80th quantile of the time series, effectively not allowing it to choose breakpoints in the first or last few years of the sample. This was done to prevent the pre- and post-period model fits from having to utilize only a very small slice of the sample, which could lead to very steep, imprecisely estimated slopes that are both noisy and a poor predictor of future trends. The model sees only total  $\text{PM}_{2.5}$  data when estimating the breakpoint. The process is implemented in the `segmented` package in R (35).

We first fit a single model for the entire United States, pooling station-year data for all available stations and producing a single breakpoint for all states, separately for annual average  $\text{PM}_{2.5}$  and extreme daily  $\text{PM}_{2.5}$  (Fig S2). We then retain the station-year resolution but fit models separately for each of nine climate regions in Fig 1, pooling all stations in each region and giving each state the resulting breakpoint in its corresponding region (Figs S3 and S4). The main breakpoint estimates are fit with station-year data limited to stations with at least 10 years of data each with over 50 observations, but results of both models are robust to increasing the temporal resolution to station-month and to various inclusion criteria that drop stations that report only intermittently or for a small number of years. Including station fixed-effects (i.e., separate intercepts for each pollution station) in the breakpoint estimation equation has no substantively or statistically meaningful effect on estimated breakpoints; inclusion results in the estimated break occurring 0.066 years earlier on average relative to a model that includes time as its only predictor. Visually, and as expected, the region-specific models modestly outperform the CONUS-wide model, particularly in the fire-heavy Western states where region-specific breakpoints suggest an earlier stagnation in total  $\text{PM}_{2.5}$ . However, these differences produce only minor changes in state-level inferences about the influence of wildfire smoke in driving total  $\text{PM}_{2.5}$  as compared to using a common CONUS-wide breakpoint (Figs S7-S8 and Tables S2 -S3).

**Estimating trends in  $\text{PM}_{2.5}$**  To estimate trends in  $\text{PM}_{2.5}$  for the early and recent periods, we fit linear panel regressions to station-year observations, pooling stations within a given region of interest and allowing intercepts and slopes to differ on either side of the prescribed breakpoint. Formally, we estimated equations of the form:

$$PM_{itps} = \alpha_{ips} + \beta_{1s}(t - t^*) \mathbb{1}_{t \leq t^*} + \beta_{2s}(t - t^*) \mathbb{1}_{t \geq t^*} + \varepsilon_{itps} \quad (5)$$

where  $t^*$  is the chosen breakpoint year. The subscript  $i$  indexes pollution station,  $t$  is the year,  $p$  the early and recent periods, and  $s$  the type of particulate matter (total or non-smoke  $\text{PM}_{2.5}$ ).

$\mathbb{1}$  is the indicator function,  $\alpha_{ips}$  represents a station-period- $\text{PM}_{2.5}$  type intercept (i.e. separate intercepts for each period for each station and  $\text{PM}_{2.5}$  type of total or non-smoke), and  $\beta_{1s}$  and  $\beta_{2s}$  are the estimates of early and recent period slopes for  $\text{PM}_{2.5}$  type  $s$ , pooled across all stations  $i$ .

Equation 5 is equivalent to running split sample regressions on pooled early or pooled recent observations for each of total and non-smoke  $\text{PM}_{2.5}$ , but the single equation version allows straightforward statistical tests on the equivalence of early and recent period slopes and total and non-smoke slopes. This equation is estimated either using all stations in CONUS, or all stations in a given state. Analysis is repeated separately for annual average  $\text{PM}_{2.5}$  and for the proportion of days where  $\text{PM}_{2.5}$  is greater than  $35\mu\text{g}/\text{m}^3$  as outcomes.

We then use estimated slopes and corresponding statistical tests to categorize states into the categories shown in Figures 2 – 3; the categories and corresponding tests are described in Table S1. We assess robustness of estimated slopes and state categorization to varying station inclusion criteria, year samples, breakpoint years, and alternative methods of fitting the pre- and post-break trends (Figs S5 - S11, Tables S2 - S4). We first consider several completeness criteria for determining which monitoring stations are retained in the estimation stage, ranging from using all stations (least restrictive) to including only stations who report over 50 days per year for at least 15 years (most restrictive), with the main specification shown in Figs 2 and 3 including stations reporting over 50 days for at least 10 years. Because our statistical model allows separate intercepts by station, differences in average pollution levels between stations are accounted for, and thus even stations that do not report for the full period can contribute useful information that will not bias trend estimates; correspondingly, we see little difference in estimates that use an unrestricted sample of stations versus a sample that restricts to stations that report in all years (Figs S8 and S11).

Next, because trends may be sensitive to the recent-sample outlier years where wildfire severity varied strongly from year-to-year, we also investigate the effect of dropping each of the last 3 years in our data (2020, 2021 and 2022). The year 2021 has the most influence on estimates, and removing it from the analysis results in 14 fewer states classified as smoke-influenced for average annual  $\text{PM}_{2.5}$  and 7 fewer states classified as smoke-influenced for portion of days where  $\text{PM}_{2.5}$  is greater than  $35\mu\text{g}/\text{m}^3$  (Tables S3 and S4). Given that VPD over western forests is a strong driver of wildfire smoke, that 2021 was a year of historically high VPD over western forests, and that future VPD averages are likely to exceed these historical extremes (Fig 4), inclusion of 2021 in the sample is arguably important for understanding recent trends in wildfire smoke. Nevertheless, sensitivity of estimates to its exclusion suggests the need to further assess wildfire smoke's contribution in coming years.

We also examine whether moving the CONUS breakpoint forward or backward by one year, to 2017 and 2015 for average annual  $PM_{2.5}$  and to 2009 and 2011 for portion of days where  $PM_{2.5} > 35 \mu g/m^3$ , or using region-specific breakpoints impacts our estimates. For average  $PM_{2.5}$ , these alternative breakpoints produce somewhat fewer classifications of smoke-influenced or smoke-caused trend reversal and more classifications of stagnation compared to our 2016 CONUS breakpoint (Table S2-S3). For extreme daily  $PM_{2.5}$ , the 2009, 2011, and regional breakpoints resulted in 2 fewer, 2 more, and 1 more classifications of smoke-influenced, respectively (Table S4).

Finally, in our main specification, we effectively fit separate models on either side of the breakpoint, including the breakpoint year in both the pre- and post-period models and allowing each model their own intercepts. We test sensitivity to slightly altering this procedure, wherein we assign the breakpoint year to the pre-break sample only. We also separately fit a piecewise regression, which constrains the intercept of the post-break and pre-break models to match in the breakpoint year. For annual average  $PM_{2.5}$ , this has a meaningful effect on estimated recent-period slopes and state categorizations, because it effectively raises the second period intercept and thus mechanically lowers the estimated second period slope (in settings where that slope is positive). We view this as a less accurate fit of the recent-period slope than if the slope and intercept are estimated on only the recent period data (which is what our preferred model does, by allowing period-specific intercepts), but we report this alternate approach for completeness.

**Climatic drivers of smoke** Building on earlier work (2), we calculate the annual average vapor pressure deficit (VPD) during the warm season (May-Sept) over forests in western US states (as defined above) and relate summertime VPD to the log of annual average smoke  $PM_{2.5}$  as measured across monitoring stations in the same states using linear regression. We chose VPD as the main climatic variable because it is frequently used as a primary fire weather index in previous research, is simple to calculate from temperature and relative humidity, and is highly correlated with other fire weather and dryness measures (2, 36, 37). To calculate average seasonal VPD, we first calculate the VPD for each grid cell of a 0.25-by-0.25 degree grid over the western US from the monthly surface temperature and relative humidity derived from GRIDMET (38). We chose to directly calculate VPD from RH and surface temperature (instead of using VPD archived in GRIDMET) to be consistent with the VPD values calculated for future climate projections (as detailed below). The average VPD over the western US is then calculated as the weighted average of VPD for each grid cell, weighted by the forest coverage percentage of each grid cell. VPD calculation is performed with R package `bigleaf`.

To quantify future change in VPD, we use the projected temperature and relative humidity from

the Coupled Model Intercomparison Project Phase 6 (CMIP6) global climate model ensemble, run under different emissions scenarios. Similar to the historical analysis, we first calculate VPD values for each climate model grid cell falling over western US forests and then calculate the annual average VPD over western US during May to September for a given model and emissions scenario. We evaluate the changes in VPD across three commonly-used climate scenarios constructed as pairs between the Shared Socio-economic Pathways (SSPs) and the Representative Concentration Pathways (RCPs): SSP1-2.6, SSP2-4.5, SSP3-7.0. Consistent with the latest IPCC report and recommendations from (39), we use SSP3-7.0 as the baseline high emission scenario, SSP2-4.5 and SSP1-2.6 as the medium and low emission scenarios. In total, we use projections from 34 global climate models (GCMs) with available temperature and relative humidity at the monthly level for the historical and three climate scenarios.

To remove potential level bias from each GCM, simulated VPD values are debiased based on the calculated difference between the simulated values in the historical simulations and the observational VPD values (1979-2014) for each GCM. To reduce the uncertainty and account for internal variability, we summarize mid-century VPD changes as the average VPD values between 2040 to 2060 for each GCM and emissions scenario. We select one ensemble variant for each of the 34 models, using the first ensemble variant of each model (“r1i1p1f1”) when possible and use the other ensemble variants if “r1i1p1f1” is not available.

**Acknowledgements** We thank members of Stanford ECHOLab for helpful comments. Some of the computing for this project was performed on the Sherlock cluster, and we would like to thank Stanford University and the Stanford Research Computing Center for providing computational resources and support that contributed to these research results. MLC was supported by an Environmental Fellowship at the Harvard University Center for the Environment. MQ was supported by a fellowship at Stanford’s Center for Innovation in Global Health.

**Data and code availability** Data and code to replicate all results in the paper will be made available upon publication.

## References

- [1] Joseph E Aldy, Maximilian Auffhammer, Maureen Cropper, Arthur Fraas, and Richard Morgenstern. Looking back at 50 years of the Clean Air Act. *Journal of Economic Literature*,

60(1):179–232, 2022.

- [2] John T Abatzoglou and A Park Williams. Impact of anthropogenic climate change on wild-fire across western US forests. *Proceedings of the National Academy of Sciences*, 113(42): 11770–11775, 2016.
- [3] Marshall Burke, Anne Driscoll, Sam Heft-Neal, Jiani Xue, Jennifer Burney, and Michael Wara. The changing risk and burden of wildfire in the United States. *Proceedings of the National Academy of Sciences*, 118(2), 2021.
- [4] Philip J Landrigan, Richard Fuller, Nereus JR Acosta, Olusoji Adeyi, Robert Arnold, Abdoulaye Bibi Baldé, Roberto Bertollini, Stephan Bose-O’Reilly, Jo Ivey Boufford, Patrick N Breyse, et al. The Lancet commission on pollution and health. *The lancet*, 391(10119): 462–512, 2018.
- [5] Crystal D McClure and Daniel A Jaffe. US particulate matter air quality improves except in wildfire-prone areas. *Proceedings of the National Academy of Sciences*, 115(31):7901–7906, 2018.
- [6] Katelyn O’Dell, Bonne Ford, Emily V Fischer, and Jeffrey R Pierce. Contribution of wildland-fire smoke to US PM<sub>2.5</sub> and its influence on recent trends. *Environmental science & technology*, 53(4):1797–1804, 2019.
- [7] Yuanyu Xie, Meiyun Lin, and Larry W Horowitz. Summer PM<sub>2.5</sub> pollution extremes caused by wildfires over the western United States during 2017–2018. *Geophysical Research Letters*, 47(16):e2020GL089429, 2020.
- [8] Marissa Childs et al. Daily local-level estimates of ambient wildfire smoke PM<sub>2.5</sub> for the contiguous US. *Environmental Science and Technology*, forthcoming, 2022.
- [9] Liji M David, AR Ravishankara, Steven J Brey, Emily V Fischer, John Volckens, and Sonia Kreidenweis. Could the exception become the rule? ‘uncontrollable’ air pollution events in the US due to wildland fires. *Environmental Research Letters*, 16(3):034029, 2021.
- [10] Peter Tschofen, Inês L Azevedo, and Nicholas Z Muller. Fine particulate matter damages and value added in the US economy. *Proceedings of the National Academy of Sciences*, 116(40):19857–19862, 2019.
- [11] Jennifer A Burney. The downstream air pollution impacts of the transition from coal to natural gas in the United States. *Nature Sustainability*, 3(2):152–160, 2020.



- [12] Joseph S Shapiro. Pollution trends and US environmental policy: Lessons from the past half century. *Review of Environmental Economics and Policy*, 16(1):42–61, 2022.
- [13] Vito MR Muggeo. Estimating regression models with unknown break-points. *Statistics in medicine*, 22(19):3055–3071, 2003.
- [14] US Environmental Protection Agency. Outdoor air quality data. . accessed from <https://www.epa.gov/outdoor-air-quality-data/download-daily-data>.
- [15] Steven J Brey, Mark Ruminski, Samuel A Atwood, and Emily V Fischer. Connecting smoke plumes to sources using hazard mapping system (HMS) smoke and fire location data over north america. *Atmospheric Chemistry and Physics*, 18(3):1745–1761, 2018.
- [16] Michael Goss, Daniel L Swain, John T Abatzoglou, Ali Sarhadi, Crystal A Kolden, A Park Williams, and Noah S Diffenbaugh. Climate change is increasing the likelihood of extreme autumn wildfire conditions across California. *Environmental Research Letters*, 15(9):094016, 2020.
- [17] Steven J Brey, Elizabeth A Barnes, Jeffrey R Pierce, Abigail LS Swann, and Emily V Fischer. Past variance and future projections of the environmental conditions driving western US summertime wildfire burn area. *Earth's future*, 9(2):e2020EF001645, 2021.
- [18] Yuanyu Xie, Meiyun Lin, Bertrand Decharme, Christine Delire, Larry W Horowitz, David M Lawrence, Fang Li, and Roland Séférian. Tripling of western US particulate pollution from wildfires in a warming climate. *Proceedings of the National Academy of Sciences*, 119(14):e2111372119, 2022.
- [19] James E Neumann, Meredith Amend, Susan Anenberg, Patrick L Kinney, Marcus Sarofim, Jeremy Martinich, Julia Lukens, Jun-Wei Xu, and Henry Roman. Estimating PM<sub>2.5</sub>-related premature mortality and morbidity associated with future wildfire emissions in the western US. *Environmental Research Letters*, 16(3):035019, 2021.
- [20] Yuzhou Wang, Joshua S Apte, Jason D Hill, Cesunica E Ivey, Regan F Patterson, Allen L Robinson, Christopher W Tessum, and Julian D Marshall. Location-specific strategies for eliminating US national racial-ethnic PM<sub>2.5</sub> exposure inequality. *Proceedings of the National Academy of Sciences*, 119(44):e2205548119, 2022.
- [21] US Environmental Protection Agency. Policy Assessment for the Reconsideration of the National Ambient Air Quality Standards for Particulate Matter, May 2022. .

- [22] US Forest Service. *Confronting The Wildfire Crisis: A Strategy for Protecting Communities and Improving Resilience in America's Forests*, FS-1187a. 2022.
- [23] US Environmental Protection Agency. *Exceptional Events Guidance: Prescribed Fire on Wildland that May Influence Ozone and Particulate Matter Concentrations*, Aug 2019. .
- [24] Emily Williams. Reimagining exceptional events: Regulating wildfires through the Clean Air Act. *Wash. L. Rev.*, 96:765, 2021.
- [25] US Environmental Protection Agency. What does the poc number refer to?, Oct 2021. Accessed from <https://www.epa.gov/outdoor-air-quality-data/what-does-poc-number-refer> on December 13, 2022.
- [26] Marshall Burke, Sam Heft-Neal, Jessica Li, Anne Driscoll, Patrick W Baylis, Matthieu Stigler, Joakim Weill, Jennifer Burney, Jeff Wen, Marissa Childs, and Carlos F Gould. Exposures and behavioral responses to wildfire smoke. *Nature Human Behaviour*, 2022.
- [27] National Oceanic and Atmospheric Administration. Hazard mapping system fire and smoke product. <https://www.ospo.noaa.gov/Products/land/hms.html#about>.
- [28] W Schroeder, M Ruminski, I Csiszar, L Giglio, E Prins, C Schmidt, and J Morisette. Validation analyses of an operational fire monitoring product: The hazard mapping system. *International Journal of Remote Sensing*, 29(20):6059–6066, 2008.
- [29] Glenn D Rolph, Roland R Draxler, Ariel F Stein, Albion Taylor, Mark G Ruminski, Shobha Kondragunta, Jian Zeng, Ho-Chun Huang, Geoffrey Manikin, Jeffery T McQueen, et al. Description and verification of the NOAA smoke forecasting system: the 2007 fire season. *Weather and Forecasting*, 24(2):361–378, 2009.
- [30] Mark Ruminski, Shobha Kondragunta, Roland Draxler, and Jian Zeng. Recent changes to the hazard mapping system. In *Proceedings of the 15th International Emission Inventory Conference*, volume 15, page 18, 2006.
- [31] EPA Particulate Matter Trends. <https://www.epa.gov/air-trends/particulate-matter-pm25-trends>. Accessed: 2022-09-01.
- [32] Shannon N Koplitz, Christopher G Nolte, George A Pouliot, Jeffrey M Vukovich, and James Beidler. Influence of uncertainties in burned area estimates on modeled wildland fire PM<sub>2.5</sub> and ozone pollution in the contiguous US. *Atmospheric environment*, 191:328–339, 2018.

- [33] Qian Di, Heresh Amini, Liuhua Shi, Itai Kloog, Rachel Silvern, James Kelly, M. Benjamin Sabath, Christine Choirat, Petros Koutrakis, Alexei Lyapustin, Yujie Wang, Loretta J. Mickley, and Joel Schwartz. An ensemble-based model of PM<sub>2.5</sub> concentration across the contiguous United States with high spatiotemporal resolution. *Environment International*, 130: 104909, Sep 2019. ISSN 01604120. doi: 10.1016/j.envint.2019.104909.
- [34] Colleen E. Reid, Ellen M. Considine, Melissa M. Maestas, and Gina Li. Daily PM<sub>2.5</sub> concentration estimates by county, zip code, and census tract in 11 western states 2008–2018. *Scientific Data*, 8(1):112, Dec 2021. ISSN 2052-4463. doi: 10.1038/s41597-021-00891-1.
- [35] Vito MR Muggeo. segmented: An r package to fit regression models with broken-line relationships. *R News*, 8(1):20–25, 2008.
- [36] Yizhou Zhuang, Rong Fu, Benjamin D Santer, Robert E Dickinson, and Alex Hall. Quantifying contributions of natural variability and anthropogenic forcings on increased fire weather risk over the western United States. *Proceedings of the National Academy of Sciences*, 118(45):e2111875118, 2021.
- [37] Piyush Jain, Dante Castellanos-Acuna, Sean CP Coogan, John T Abatzoglou, and Mike D Flannigan. Observed increases in extreme fire weather driven by atmospheric humidity and temperature. *Nature Climate Change*, 12(1):63–70, 2022.
- [38] John T Abatzoglou. Development of gridded surface meteorological data for ecological applications and modelling. *International Journal of Climatology*, 33(1):121–131, 2013.
- [39] Zeke Hausfather and Glen P Peters. Emissions—the ‘business as usual’ story is misleading. *Nature*, 577(7792):618–620, 2020.

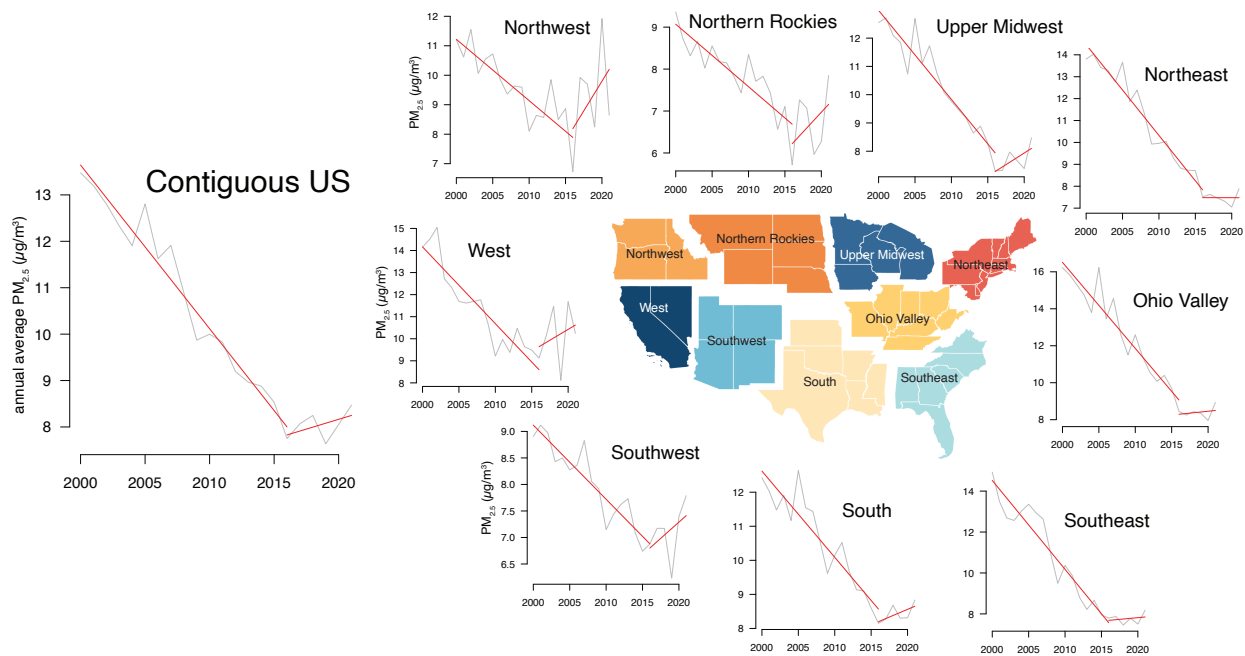
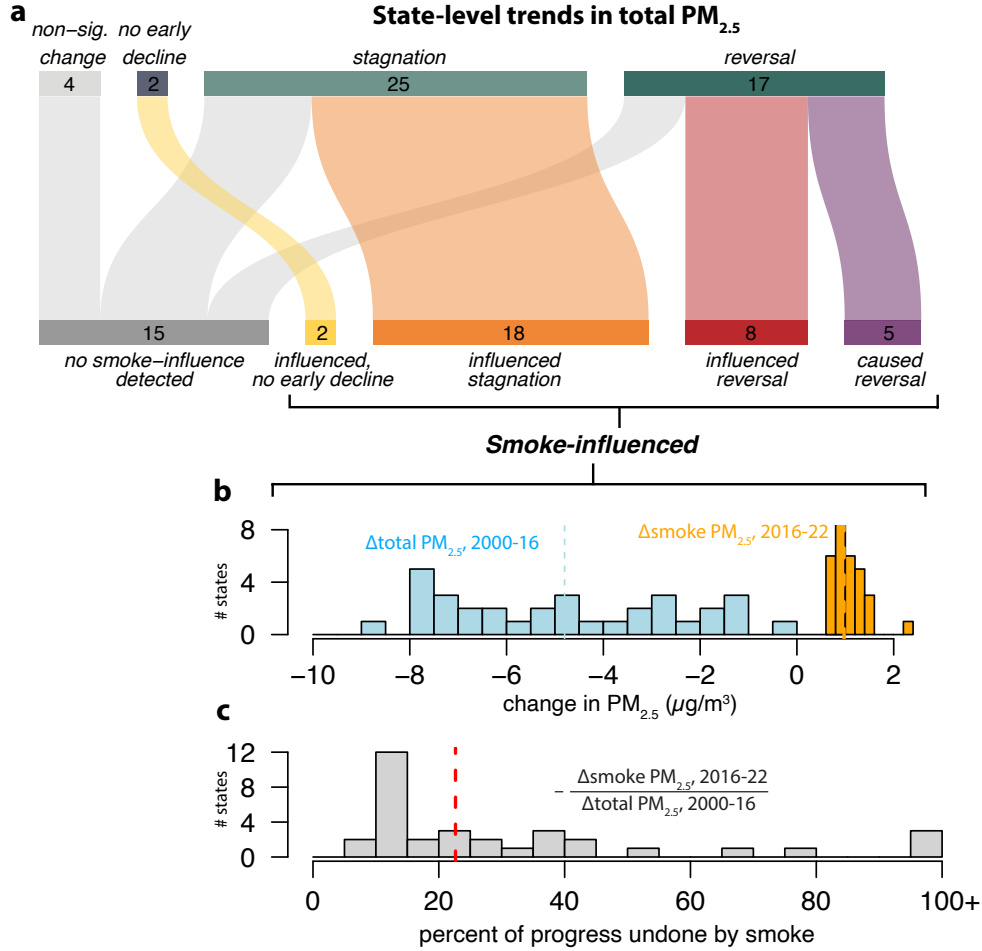


Figure 1: **National and regional trends in ambient concentrations of  $PM_{2.5}$  show steady declines through 2016 and then stagnation or reversal.** Grey lines in each subplot are EPA-estimated annual average regional concentrations of  $PM_{2.5}$  averaged over monitoring stations reporting consistently over the period in each US climate region (31). Red lines are linear fits to each region's annual average time series, with separate fits for 2000-2016 and 2016-2021.



**Figure 2: Improvements in total PM<sub>2.5</sub> have slowed or reversed in most states, and smoke is a significant influence in the majority.** **a.** Classification of states by trend in total PM<sub>2.5</sub> in 2000-2016 versus 2016-2022; non-declining are states where first period PM<sub>2.5</sub> is not declining (“no early decline”) or where trends in early and recent periods are not statistically different (“non-sig. change”), “stagnation” includes states where declines are slower ( $p < 0.05$ ) in the recent period relative to the early period but not significantly negative, and “reversal” includes states where early trend was significantly negative and recent trend was significantly positive. Numbers give states in each category, out of 48 CONUS states. Alluvial plot then shows the count of states in each of these categories that are smoke-influenced in the recent period, defined as total PM<sub>2.5</sub> having a significantly ( $p < 0.05$ ) larger slope than estimated non-smoke PM<sub>2.5</sub>. A “caused reversal” is a recent-period trend in total PM<sub>2.5</sub> that would have been negative absent smoke. **b.** In the 34 smoke-influenced states, the distribution of change in total PM<sub>2.5</sub> during early period (blue), and change in smoke PM<sub>2.5</sub> during the recent period (orange); dotted lines are medians across states. **c.** Ratio of recent-period smoke-attributed PM<sub>2.5</sub> increase to early-period total PM<sub>2.5</sub> decline, representing the percent of early period progress in reducing total PM<sub>2.5</sub> concentrations that was undone by smoke in the recent period; dotted line is the median across states.

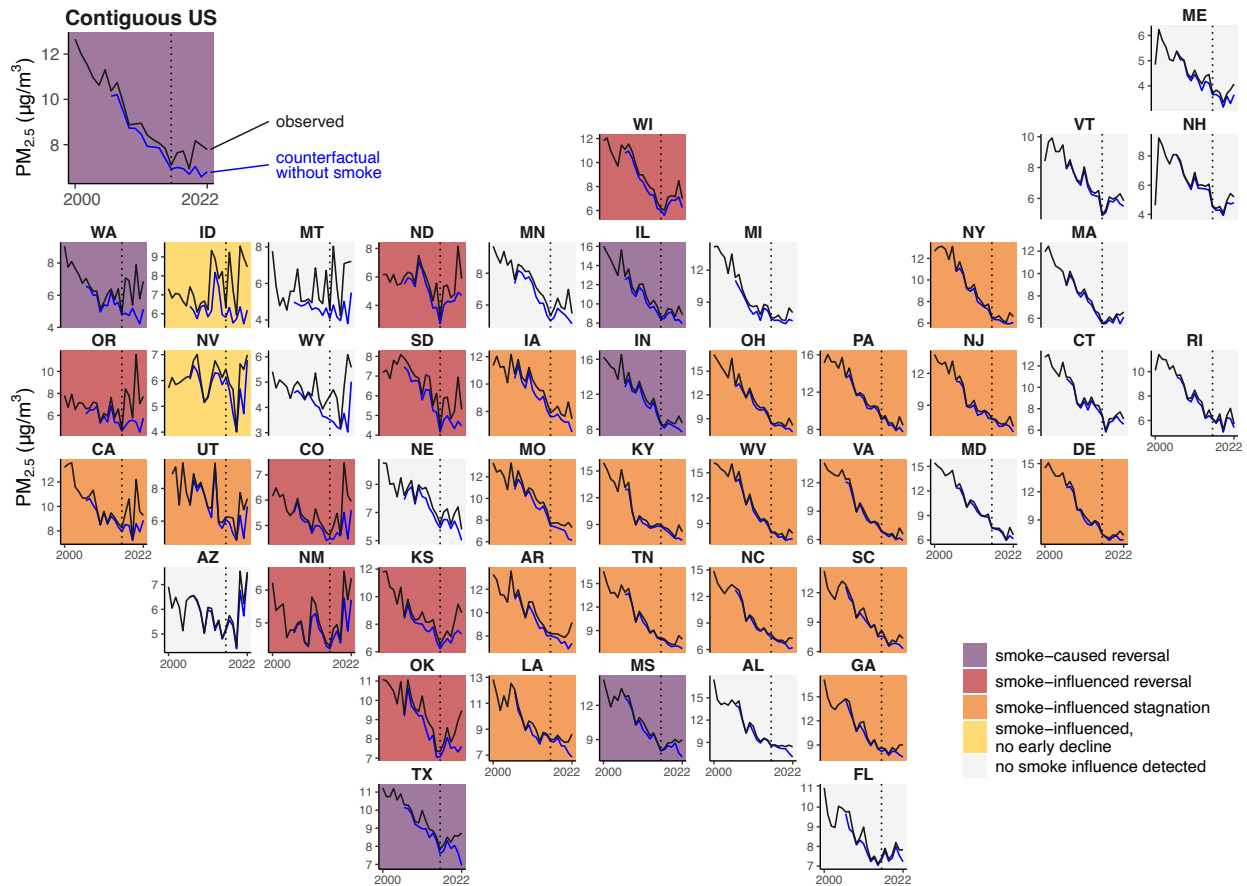
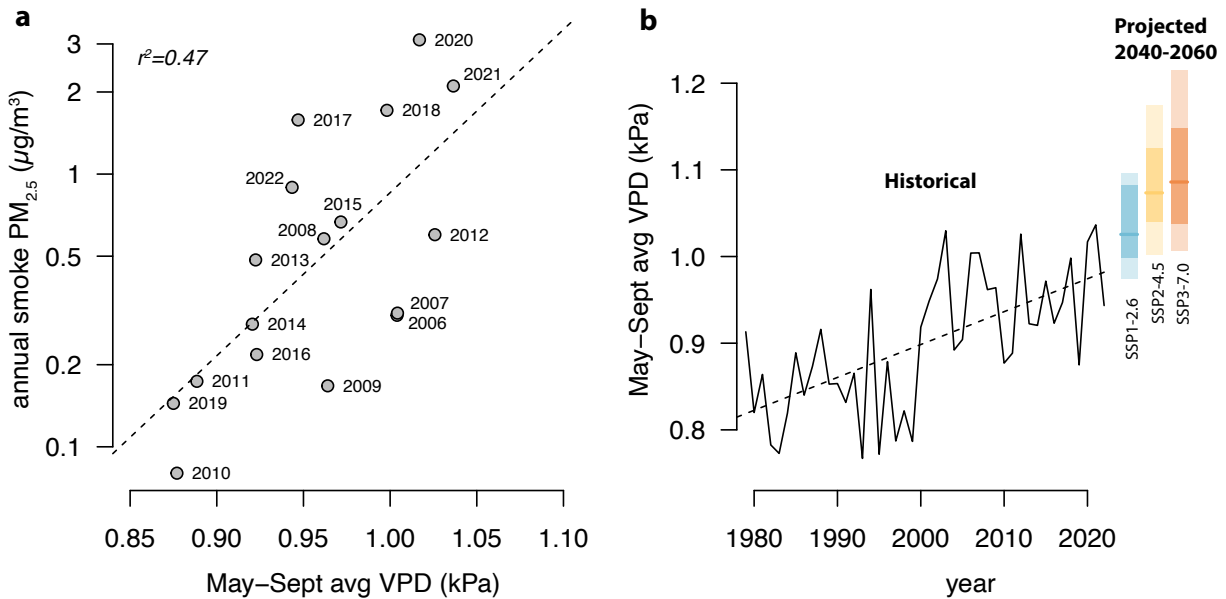


Figure 3: **The influence of wildfire smoke on recent trends in average  $PM_{2.5}$  is largest in the Western states, but extends to the Great Plains, Midwest, and parts of the Southeast.** Lines show annual averages in the state for observed total  $PM_{2.5}$  (black) and counterfactual estimated  $PM_{2.5}$  without smoke (blue). State averages lines shown in the panels are calculated from stations with at least 15 years of data, each with over 50 observations per year. Vertical dashed line shows the CONUS-wide break year (2016) used in the main specification. Panels are colored by smoke-influenced classification, which is determined using regression on station-year level data pooled within each state. Smoke-influence classifications match those used in Fig. 2.



**Figure 4: Climate is a strong historical driver of interannual variation in smoke exposure, and projected mid-century changes in climatic drivers exceed recent historical extremes.**

**a.** Interannual variation in summertime (May-Sept) vapor pressure deficit (VPD) averaged over western forests is a strong predictor of annual variation in average smoke  $PM_{2.5}$  variation across the US West, 2006-2022 ( $r^2=0.47$ ); smoke  $PM_{2.5}$  is a simple average of daily smoke  $PM_{2.5}$  over all reporting stations in the US West in a given year, and dotted line is linear regression fit. **b.** Historical and projected mid-century changes in summertime VPD over western forests. Rectangles at right show projected mid-century (2040-2060) average summertime VPD from an ensemble of 34 global climate models run under the listed emissions scenarios and debiased to match observed VPD values in a common 1979-2014 sample; lighter rectangles are 10-90th percentiles, darker rectangles are interquartile range, and solid horizontal line is ensemble median. Mid-century median projected values across all emissions scenarios exceed recent historical extremes, suggesting smoke  $PM_{2.5}$  is likely to continue to increase absent additional intervention.

## **Supplemental Information**



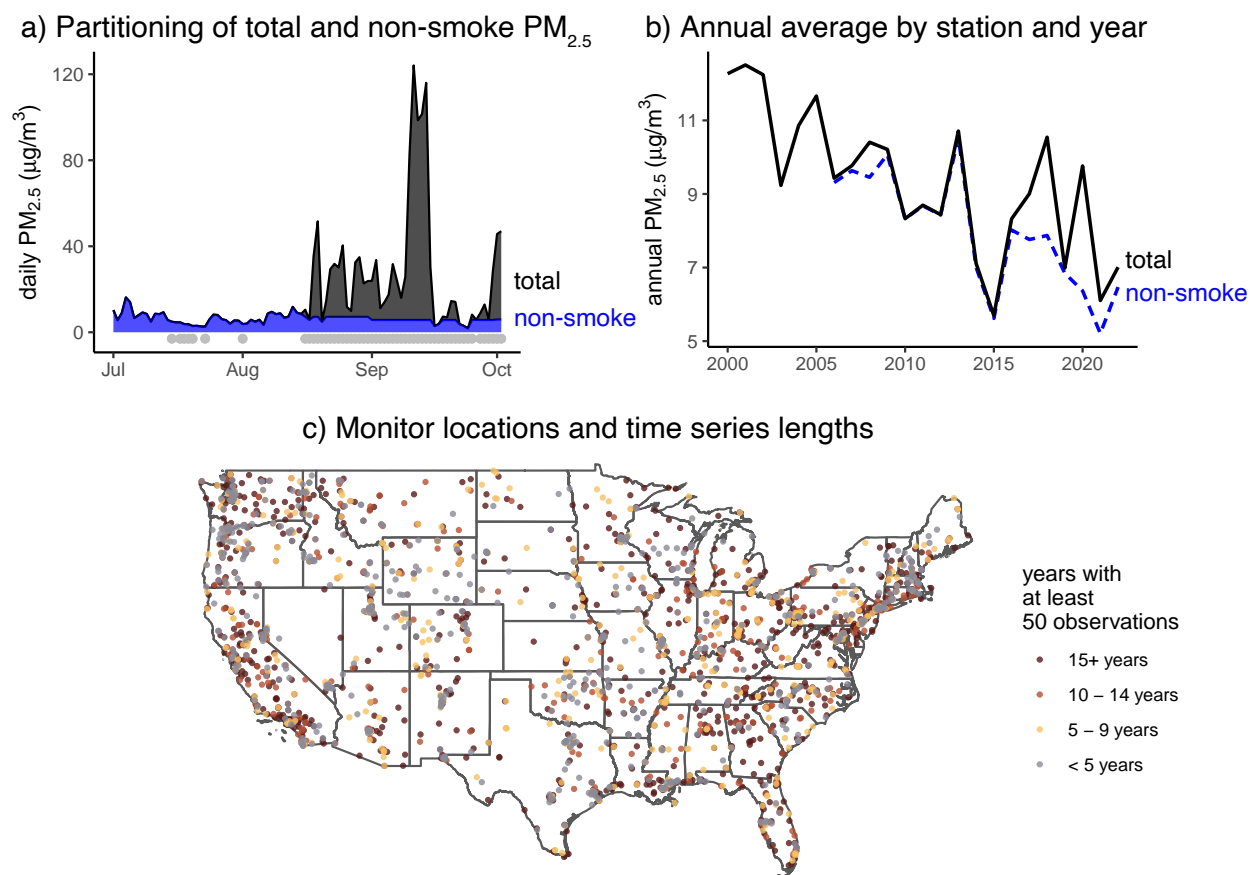


Figure S1: **Pollution stations and method used to construct non-smoke  $PM_{2.5}$  estimates.** **a.** Example of total and non-smoke partitioning for a single station in CA in 2020. On days without a smoke plume overhead (no grey points), all  $PM_{2.5}$  is assumed to be from non-smoke sources. On days with a plume overhead (grey points),  $PM_{2.5}$  above the non-smoke month- and station-specific 3-year median is attributed to smoke and only  $PM_{2.5}$  levels up to the median are attributed to non-smoke (blue). **b.** Annual average total and non-smoke  $PM_{2.5}$  for the same station is produced by aggregating daily total observed  $PM_{2.5}$  (black) and the daily estimates of non-smoke  $PM_{2.5}$  (blue). **c.** Locations of  $PM_{2.5}$  stations throughout the contiguous US. Stations are colored by the number of years with at least 50 observations.

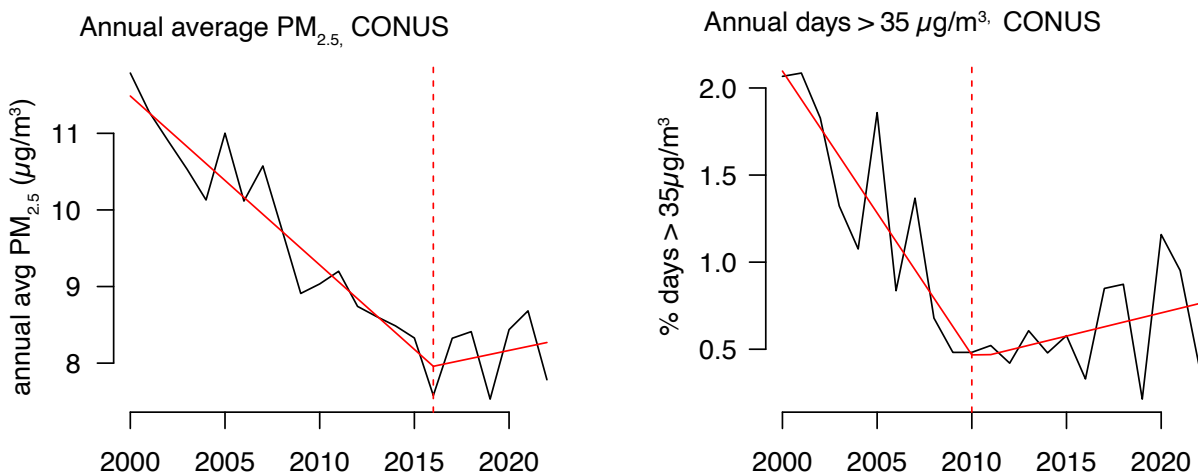
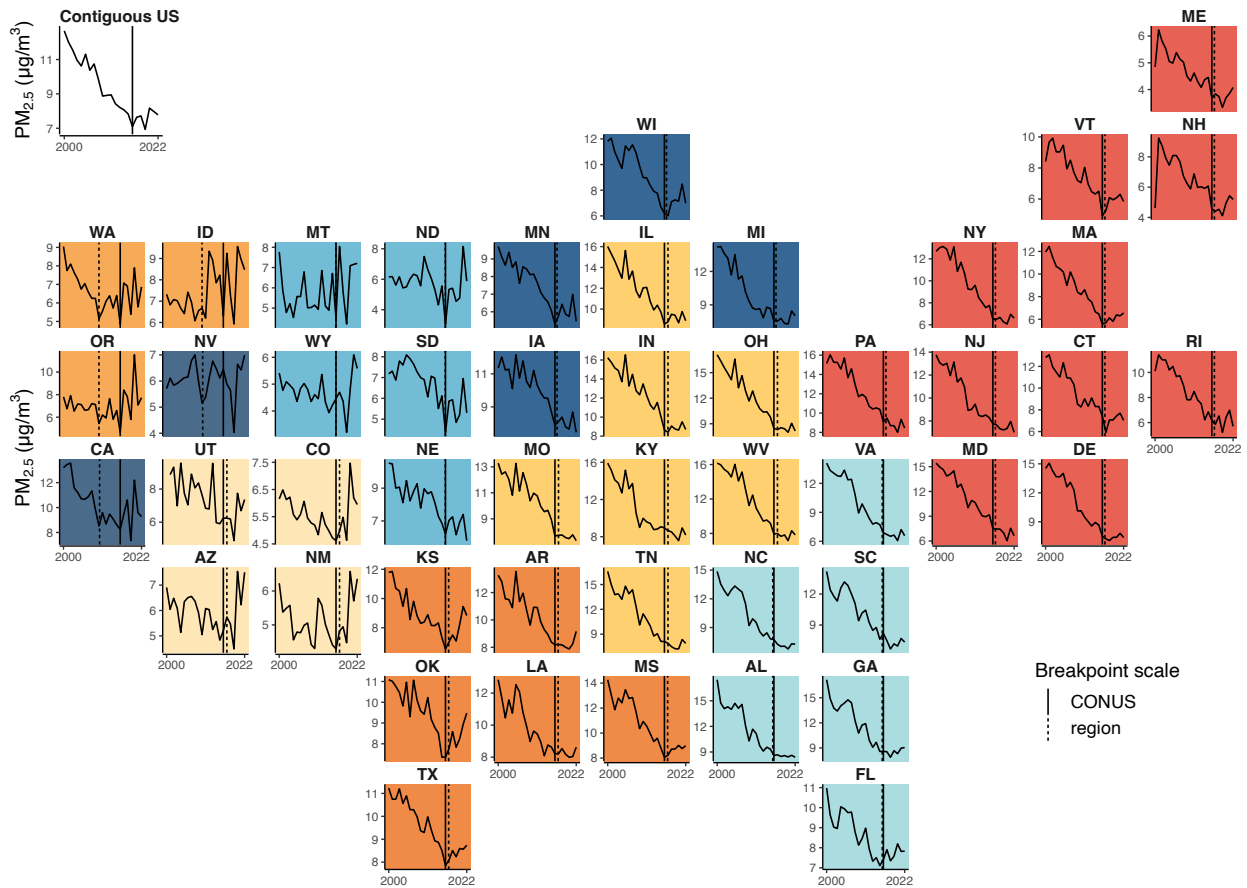


Figure S2: **Breakpoint estimates for annual average PM<sub>2.5</sub> and extreme PM<sub>2.5</sub> days, pooling data across CONUS.** Black line is pollution level averaged across stations, vertical dotted line provides the estimated break point in each time series following approach in ref (13) and described in Methods, and red solid lines show the estimated slopes on either side of the breakpoint.



**Figure S3: Breakpoint year estimates for annual average  $PM_{2.5}$  in each climate region.** Breakpoints are estimated pooling all stations in each US climate region (each denoted by a different color), and then are visualized over the  $PM_{2.5}$  time series in each state in that region. State small multiples are colored by climate region matching those from Fig. 1. Dashed vertical lines show the region-specific estimated breakpoints, while solid vertical lines show the the CONUS-wide breakpoint. Lines show the state average total  $PM_{2.5}$  matching the total  $PM_{2.5}$  shown in Fig. 3, as calculated from stations with at least 15 years of data, each with 50 observations per year.

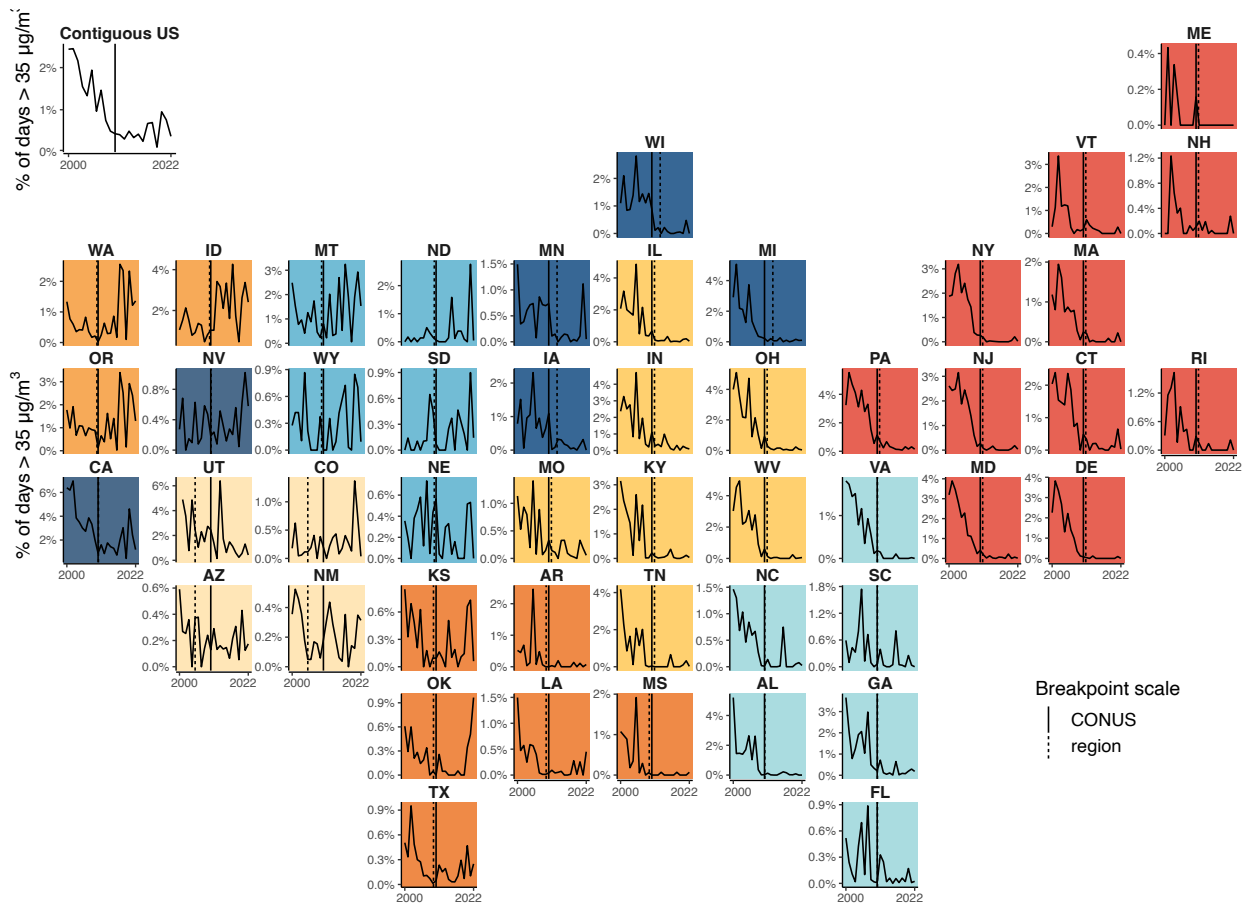


Figure S4: Breakpoint year estimates for the proportion of days in each year with PM<sub>2.5</sub> concentrations above 35 µg/m<sup>3</sup> in each climate region.. Breakpoints are estimated pooling all stations in each region (regions denoted by the different colors), and then are visualized over the state-averaged proportion of days >35 µg/m<sup>3</sup>. Lines are as in Fig S3.

Table S1: **Definition of trend groupings.** We subdivide states into “stagnation” states and “reversal” states based on comparison of trends in total  $PM_{2.5}$  between early and recent periods, and then subdivide those based on whether they were smoke-influenced. The  $\beta$ 's refer to period-specific estimated slopes on  $PM_{2.5}$  :  $\beta_1$  and  $\beta_2$  are first- and second-period slopes on total  $PM_{2.5}$  ,  $\beta_1^*$  and  $\beta_2^*$  are corresponding period slopes for non-smoke  $PM_{2.5}$  . Strong inequalities ( $>$  or  $<$ ) have to be statistically significant ( $p < 0.05$ ) for condition to be met.

Group	Conditions on slopes				In words
	$\beta_1$	$\beta_2$	$\beta_1^*$	$\beta_2^*$	
<b><u>Trends in total <math>PM_{2.5}</math></u></b>					
Stagnation	$< 0$	$\leq 0 \ \& \ > \beta_1$			<i>Total <math>PM_{2.5}</math> declined in the first period but declined more slowly or was flat in second period.</i>
Reversal	$< 0$	$> 0$			<i>Total <math>PM_{2.5}</math> declined in the first period but increased in the second period.</i>
<b><u>Influence of smoke <math>PM_{2.5}</math></u></b>					
Smoke-influenced Stagnation	$< 0$	$\leq 0 \ \& \ > \beta_1$		$< \beta_2$	<i>A stagnation where recent period <math>PM_{2.5}</math> would have declined more quickly without smoke.</i>
Smoke-caused Reversal	$< 0$	$> 0$		$< 0$	<i>A reversal where second-period total <math>PM_{2.5}</math> would have declined absent smoke.</i>
Smoke-influenced Reversal	$< 0$	$> 0$		$< \beta_2$	<i>A reversal where second period total <math>PM_{2.5}</math> would not have declined absent smoke, but increases would have been at a lower rate.</i>
Smoke-influenced, no early decline	$\geq 0$			$< \beta_2$	<i>Smoke influenced total <math>PM_{2.5}</math> trends in the second period, but there was no detectable decline in total <math>PM_{2.5}</math> during the first period.</i>
Smoke influence not detected				$= \beta_2$	<i>We did not detect an influence of smoke on total <math>PM_{2.5}</math> trends.</i>

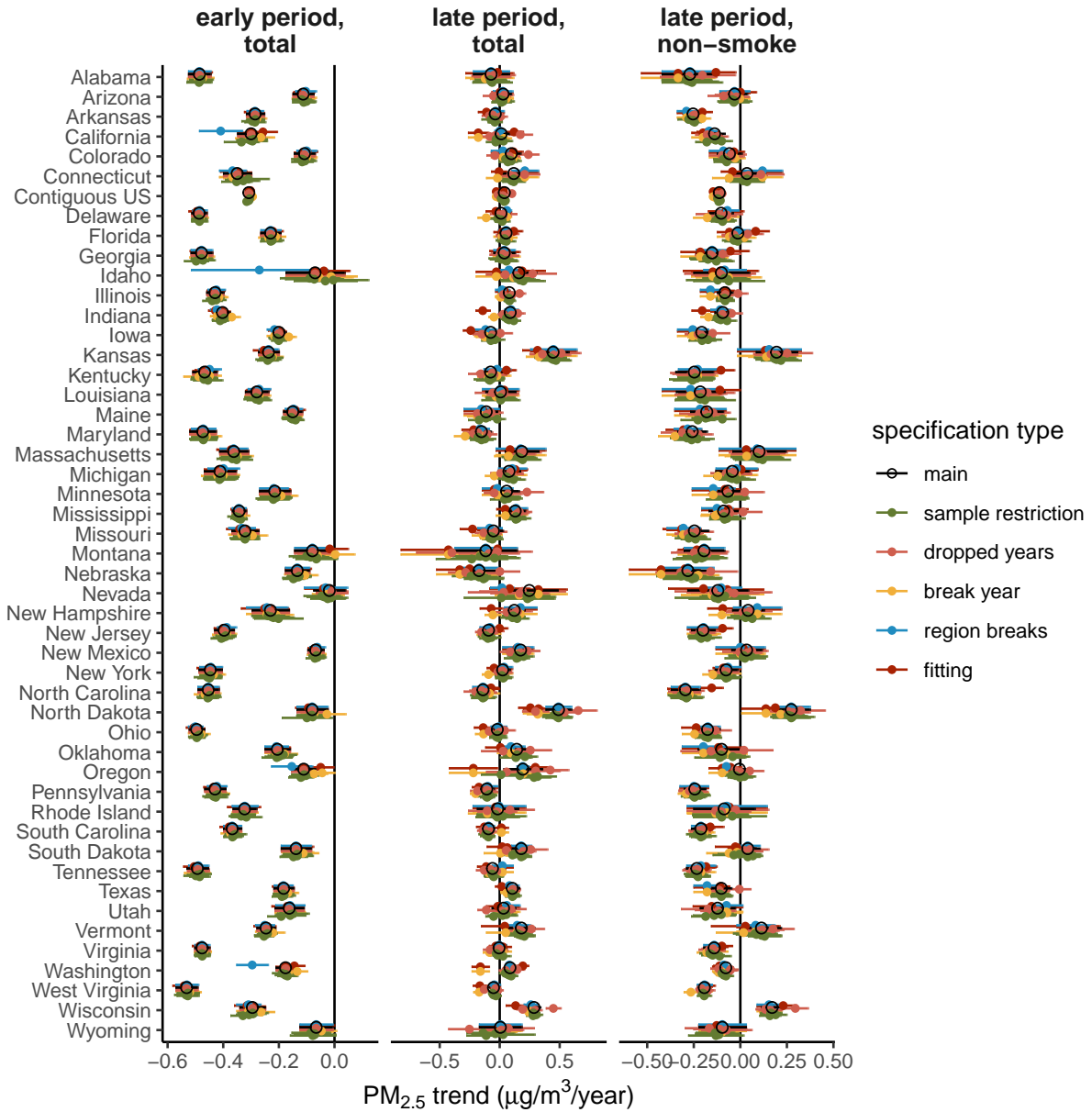


Figure S5: Sensitivity of slope coefficient estimates for early and recent-period total PM<sub>2.5</sub> and recent-period non-smoke PM<sub>2.5</sub>. Black line and circle show our main estimates, and colors show estimates under alternate station or year samples, break years, region breaks, or approach to model fitting.

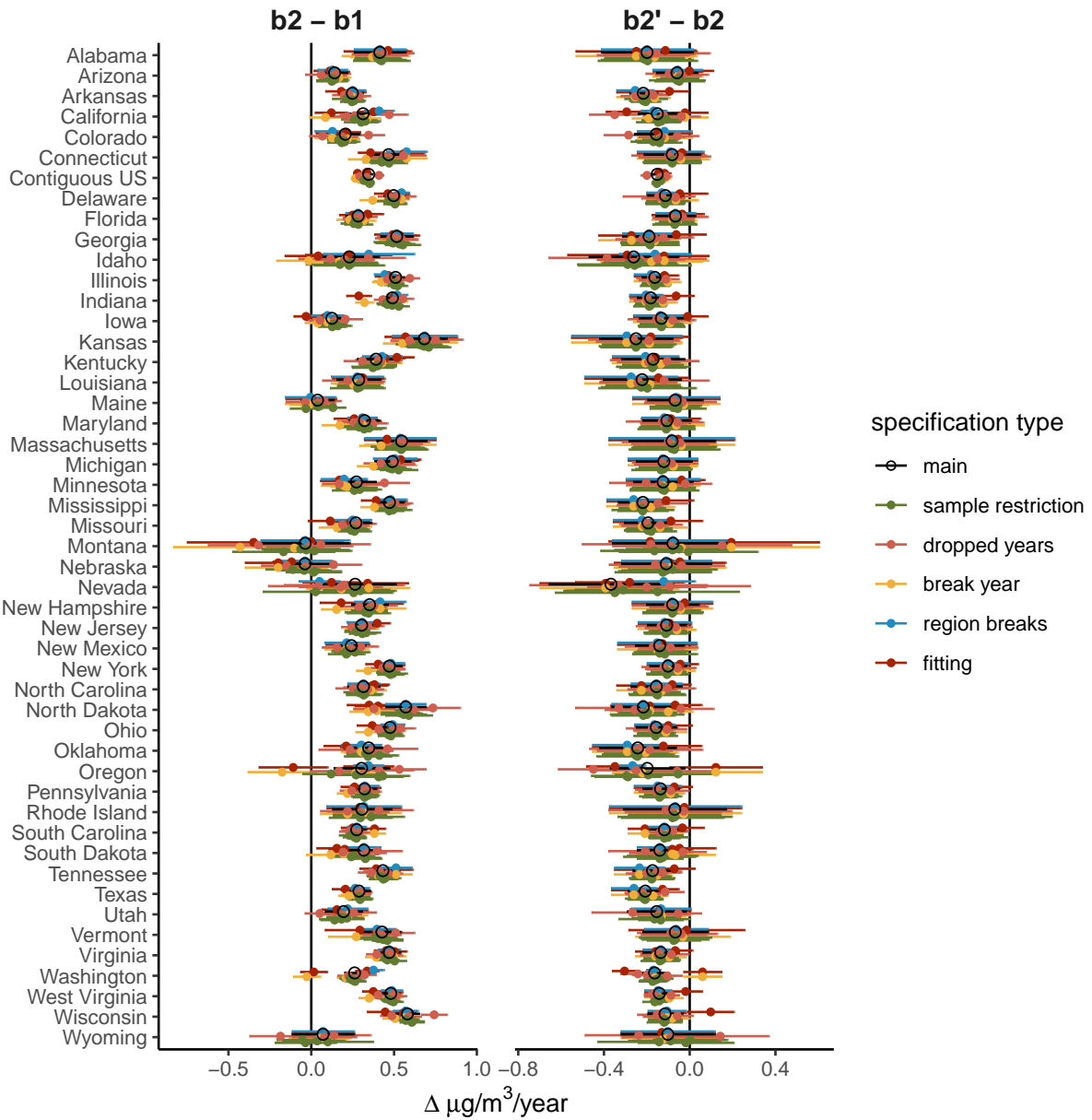


Figure S6: **Sensitivity of estimated differences in slope coefficients used to classify states.** Left column shows differences in early and recent period total PM<sub>2.5</sub> slopes, and the confidence interval on estimated differences, that are used to classify states into stagnating/reversing categories. Right columns shows differences in recent period total PM<sub>2.5</sub> and non-smoke PM<sub>2.5</sub> slopes that are used to classify states as smoke-influenced. Colors are as in Figure S5.

**Table S2: Counts of states in different total PM<sub>2.5</sub> -trend classifications, under different sample restrictions and/or statistical specifications.** Main sample uses station-years that report at least 50 days in for 10 years, with the year break in 2016. Other samples are as listed, e.g. “10yrs, 100obs” restricts to stations that report at least 100 days in each of at least 10 years. “Drop” samples are those that drop individual years. “No dup. break yr” is a sample that does not duplicate the break year. Specifications that identify a break year otherwise match the main specification, “regional breaks” uses breaks specific to each region shown in Fig S3, and “piecewise” forces segments on either side of the break year to intersect at the break year.

<i>Specification or Sample</i>	reversal	stagnation	acceleration	non-sig. change	no sig. early decline
Main	17	25	0	4	2
All obs	14	27	0	5	2
5yrs, 50obs	16	26	0	4	2
15yrs, 50obs	16	27	0	1	4
10yrs, 100obs	17	25	0	2	4
break in 2015	9	30	0	5	4
break in 2017	11	27	0	5	5
drop 2020	15	26	0	5	2
drop 2021	10	28	1	7	2
drop 2022	19	23	0	4	2
no dup. break yr	11	28	0	7	2
piecewise	10	30	1	4	3
regional breaks	14	28	0	5	1



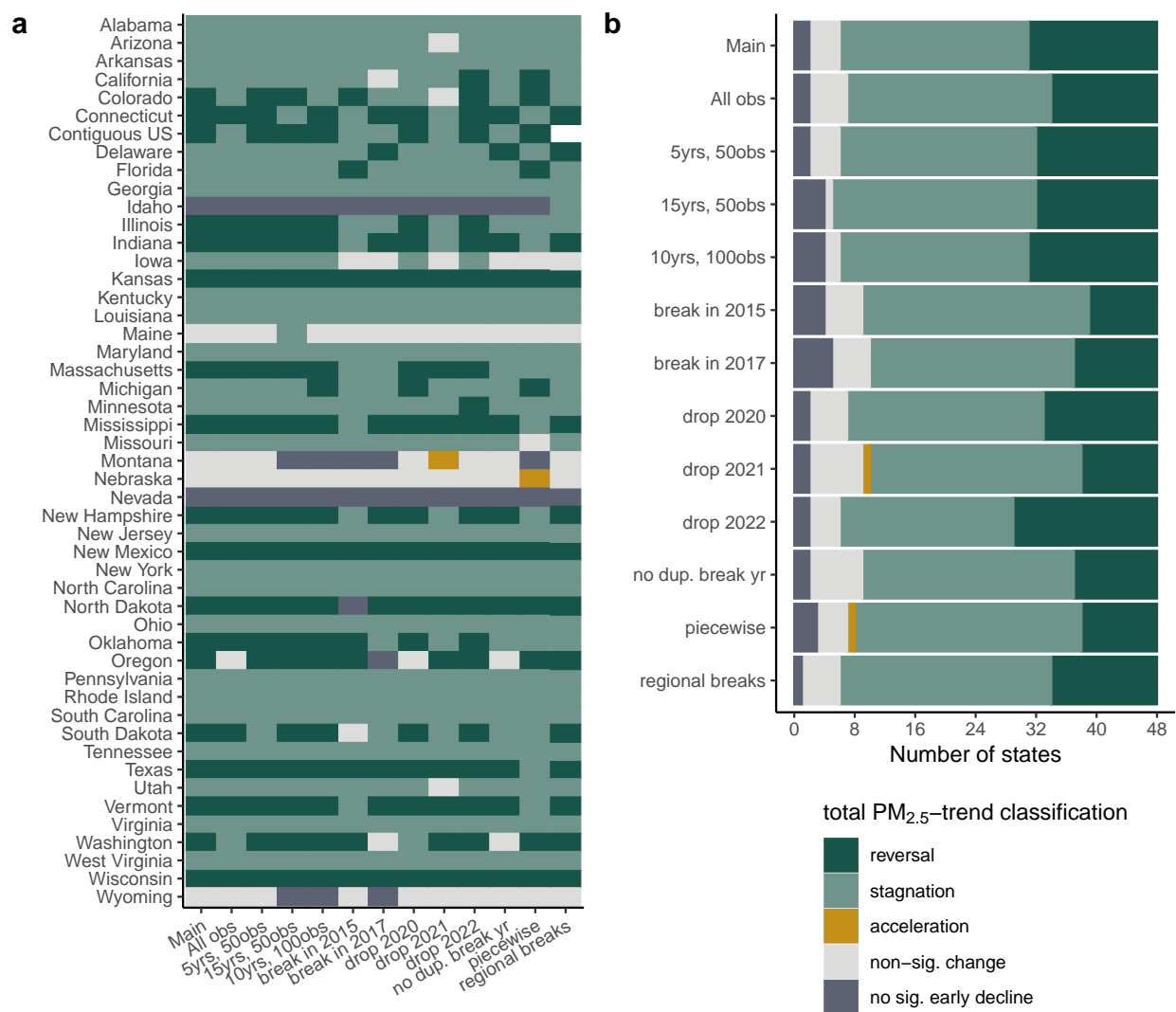


Figure S7: **Sensitivity of PM<sub>2.5</sub> trend classification to model specification, station sample, and year sample.** Left plot shows state-specific categorization under the alternative estimates, right plot shows counts of states in each classification. Model specifications and samples match those in Table S2.

**Table S3: Counts of states in different smoke-influence classifications, under different sample restrictions and/or statistical specifications.** Samples and specifications are as in Table S2.

<i>Specification or Sample</i>	<b>Smoke-influenced?</b>		<b>Influenced</b>				
	no	yes	caused reversal	influenced reversal	influenced stagnation	influenced, no early dec.	influenced, no sig. trend
Main	15	33	5	8	18	2	0
All obs	15	33	4	5	22	2	0
5yrs, 50obs	14	34	6	6	20	2	0
15yrs, 50obs	18	30	5	8	16	1	0
10yrs, 100obs	18	30	5	6	18	1	0
break in 2015	23	25	2	5	17	1	0
break in 2017	23	25	4	3	16	1	1
drop 2020	15	33	4	7	21	1	0
drop 2021	29	19	2	3	14	0	0
drop 2022	20	28	2	13	12	1	0
no dup. break yr	23	25	4	3	16	1	1
piecewise	34	14	2	4	6	2	0
regional breaks	20	28	6	4	17	0	1

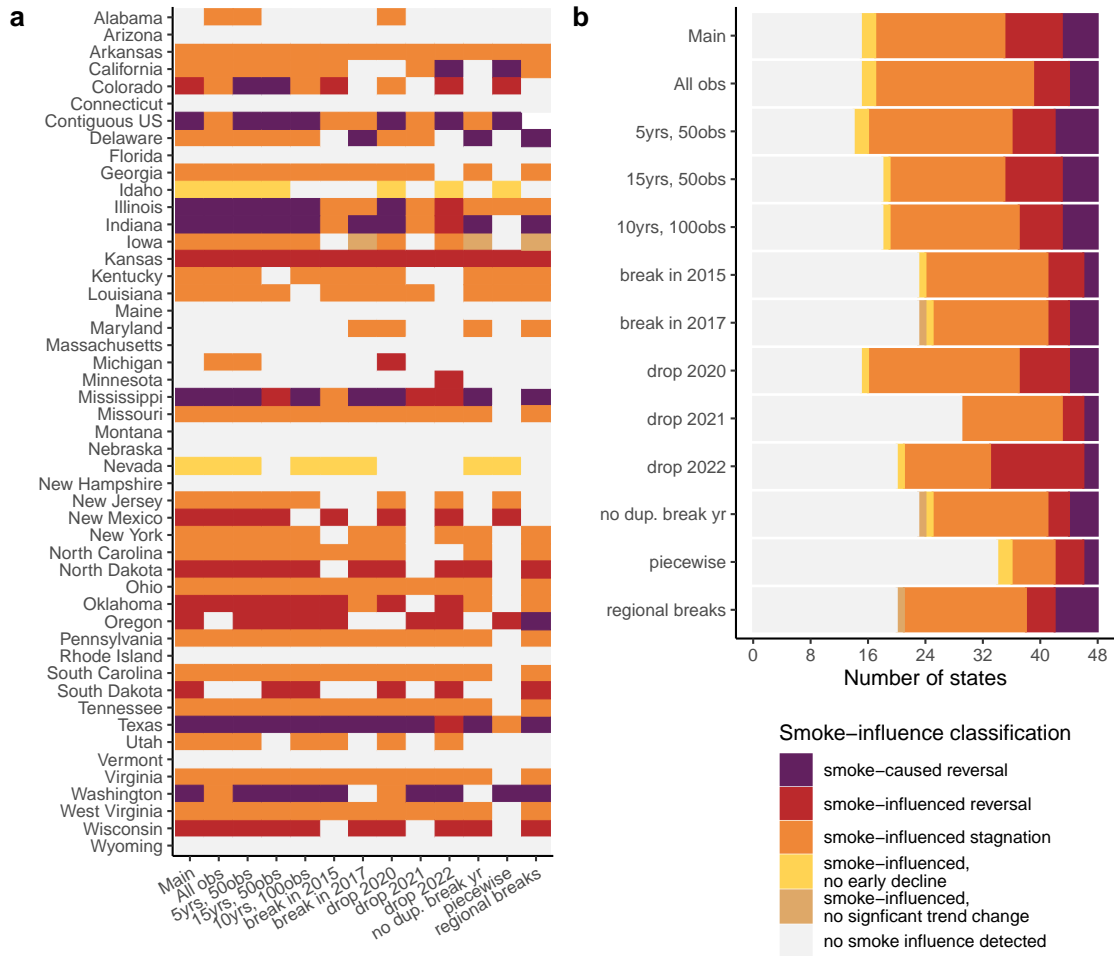


Figure S8: **Sensitivity of smoke-influence classification to model specification.** Left plot shows state-specific categorization under the same alternative estimates used in above analyses, right plot show counts of states in each classification. Model specifications and samples match those in Table S2.

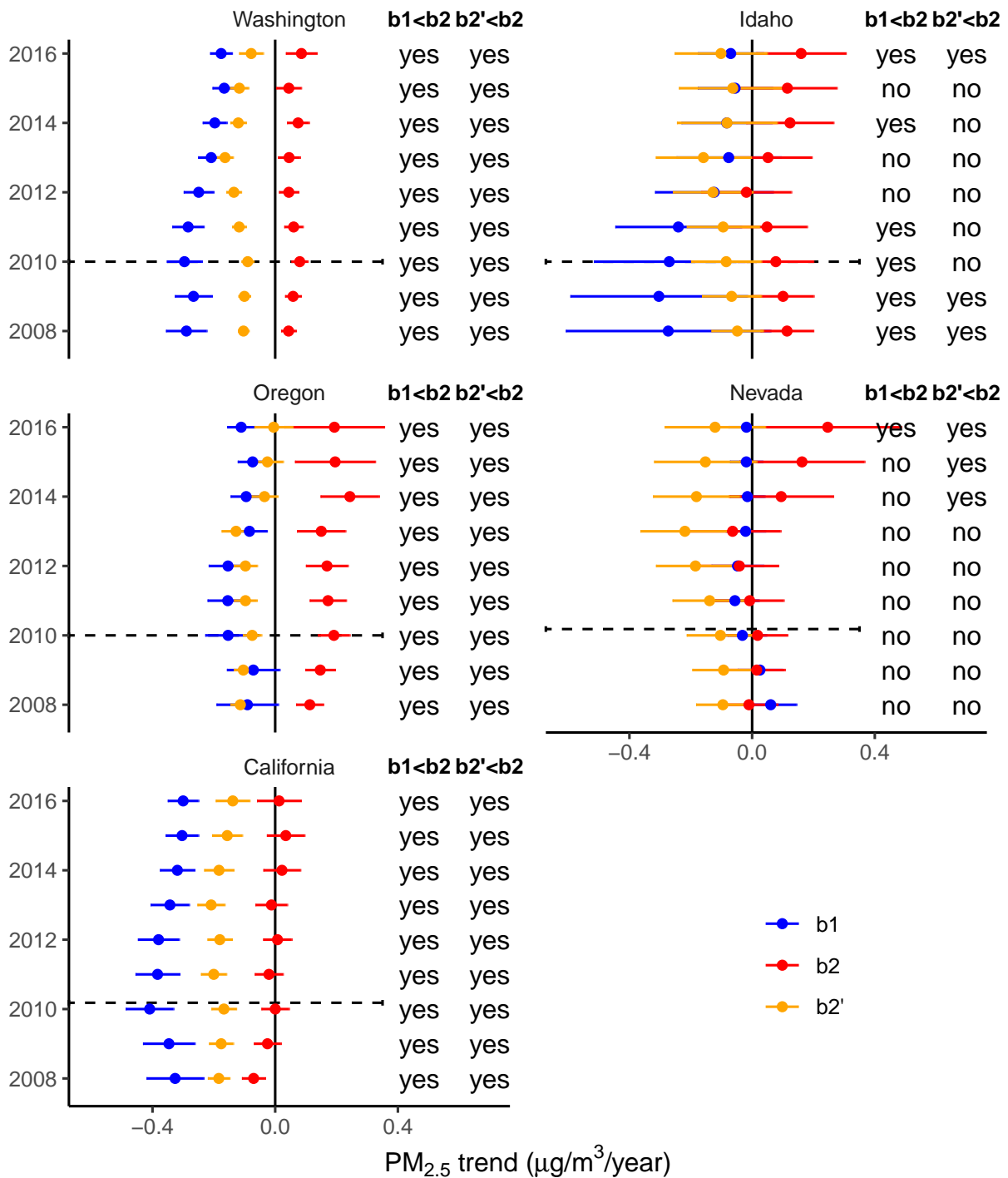


Figure S9: **Coefficient estimates in western states are largely robust to using earlier break point years.** Blue dots and whiskers show estimate and confidence intervals on early period total PM<sub>2.5</sub>, red dots on recent period total PM<sub>2.5</sub>, and orange dots on recent period non-smoke PM<sub>2.5</sub>. Horizontal dashed line shows the estimated region-specific breakpoint. Text entries in columns at right on each panel test, respectively, whether early and recent total PM<sub>2.5</sub> slopes are different and whether recent period total and non-smoke PM<sub>2.5</sub> slopes are different.

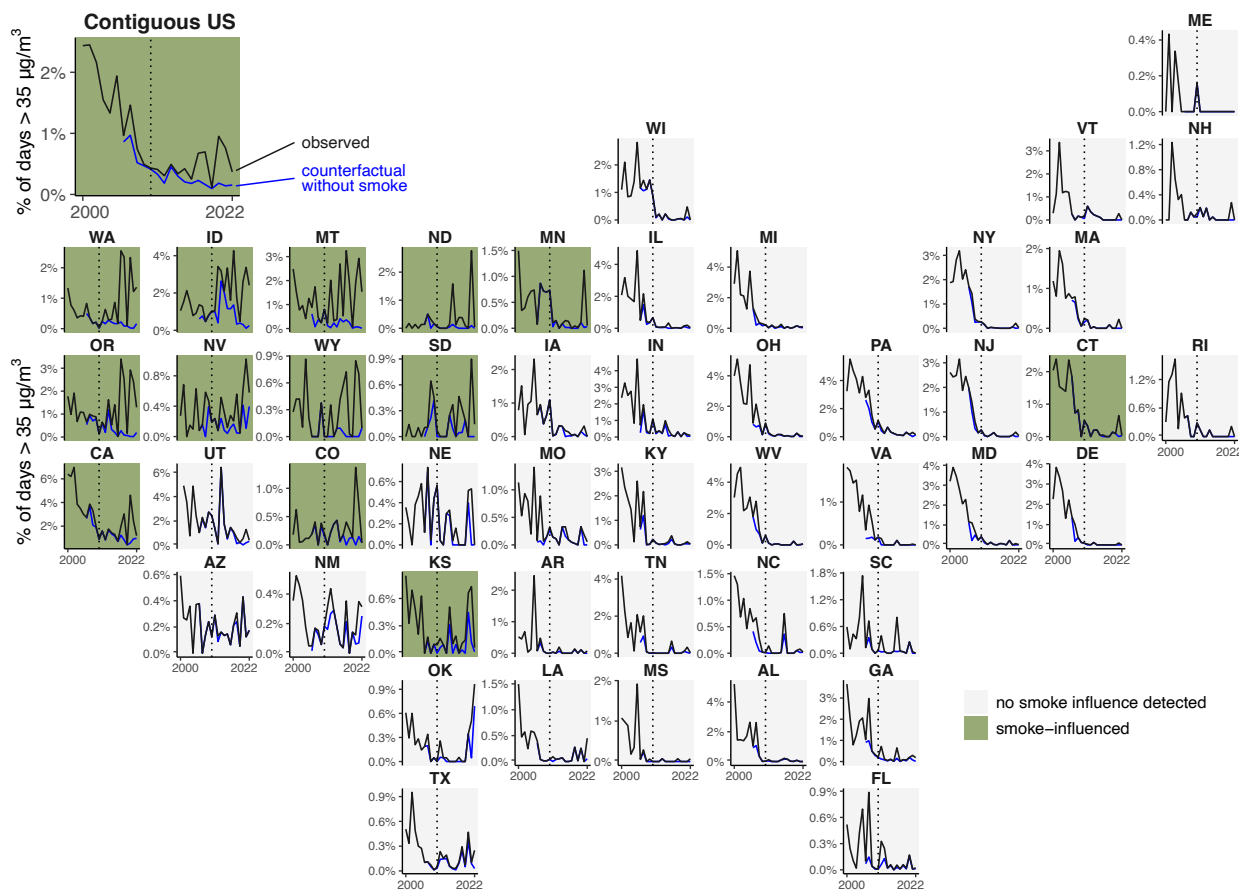


Figure S10: **Influence of wildfire smoke on daily PM<sub>2.5</sub> extremes is mainly concentrated in states in the West, Northwest, and Great Plains.** Black lines in each plot show percent of days in each state-year where PM<sub>2.5</sub> values exceed 35µg/m<sup>3</sup>, calculated using the sample of stations with over 50 observations in at least 15 years, as in Fig 3. Blue lines show estimated percent of days that exceed 35µg/m<sup>3</sup> after smoke PM<sub>2.5</sub> has been removed. Vertical dotted line indicates CONUS-wide estimated breakpoint (2010).

Table S4: **Count of states where trends in the annual proportion of extreme ( $>35\mu\text{g}/\text{m}^3$ ) days post-2010 are estimated to be wildfire-smoke influenced.** Specifications and samples are as in Table S2.

<i>Specification or Sample</i>	no smoke influence detected	smoke-influenced
Main	35	13
All obs	35	13
5yrs, 50obs	35	13
15yrs, 50obs	36	12
10yrs, 100obs	35	13
break in 2009	37	11
break in 2011	33	15
drop 2020	33	15
drop 2021	42	6
drop 2022	35	13
no dup. break yr	33	15
piecewise	36	12
regional breaks	34	14

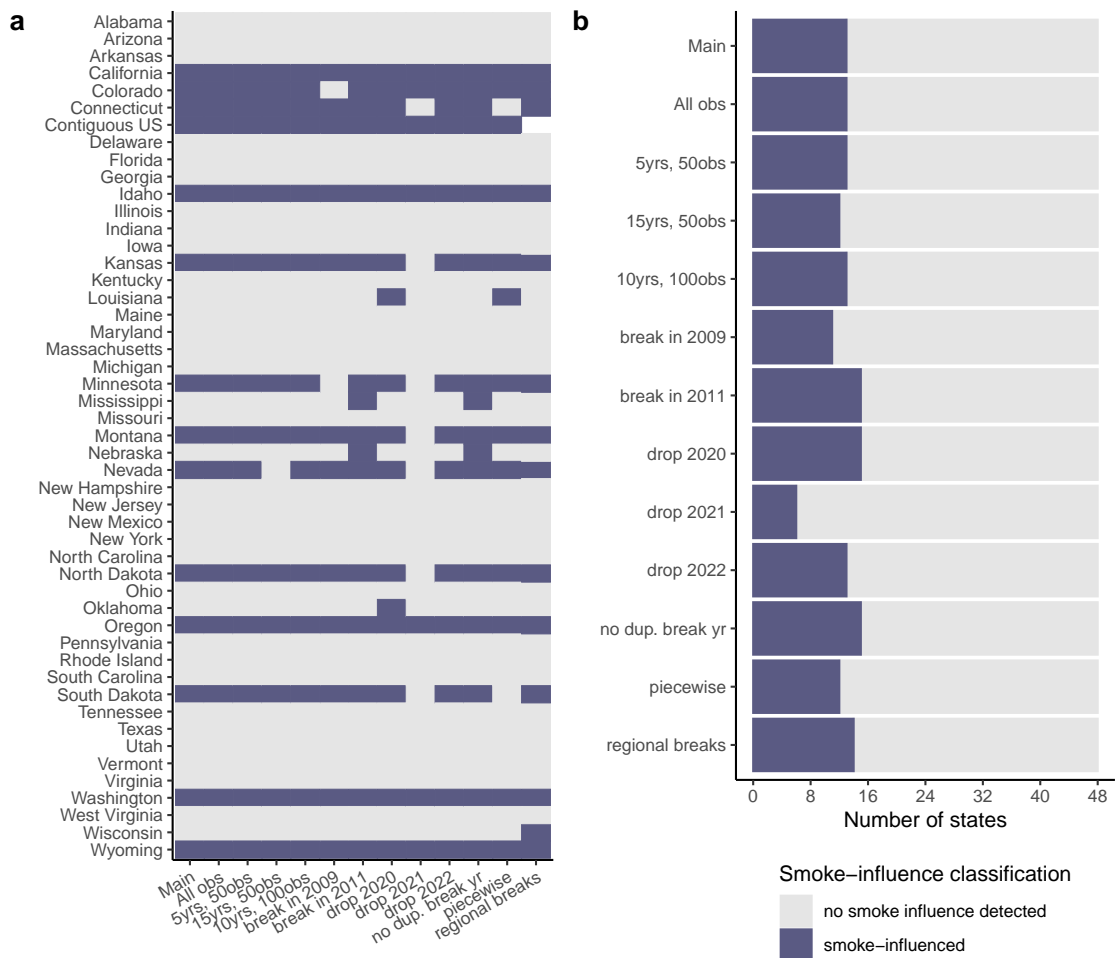


Figure S11: **Sensitivity of smoke-influence classification on portion of extreme days (> 35 μg/m<sup>3</sup>) to model specification.** Left plot shows state-specific categorization under the same alternative estimates, right plot show counts of states in each classification. Model specifications and samples match those in Table S2.

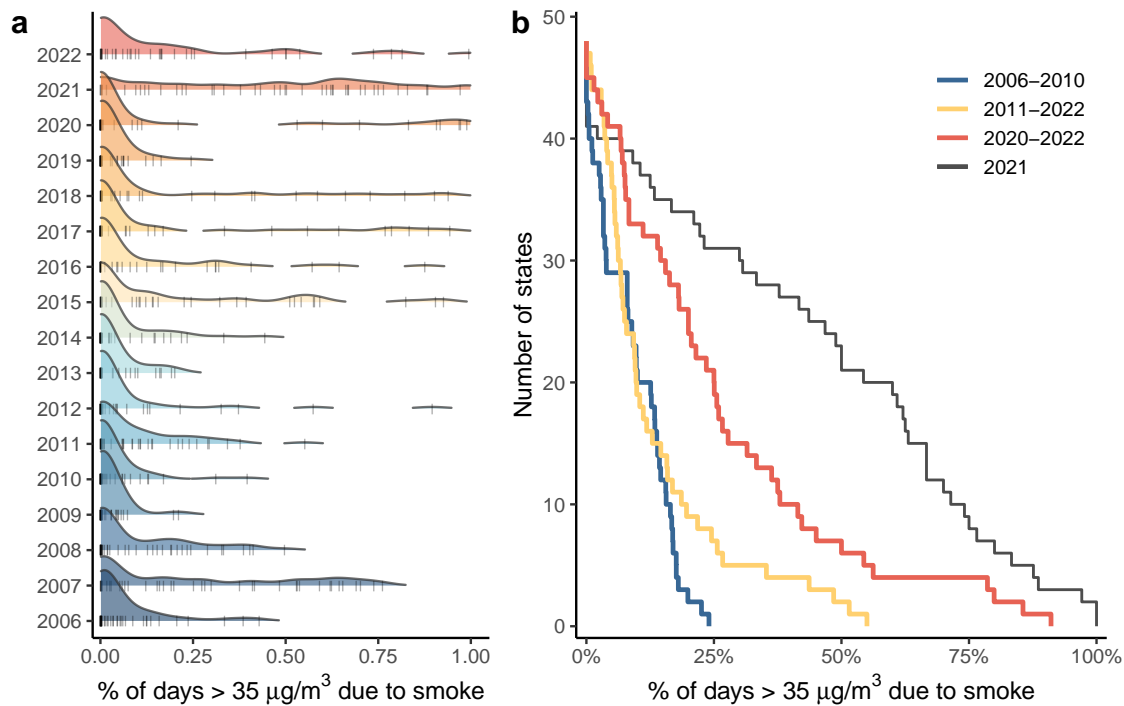


Figure S12: **Distribution of proportion of extreme days due to wildfire smoke by state.** **a.** Density plots show, for each year, the distribution across CONUS states of the proportion of days above  $35\mu\text{g}/\text{m}^3$  due to smoke, i.e. days that would have had concentrations  $<35\mu\text{g}/\text{m}^3$  were smoke not present. Tick marks show values for individual states. **b.** Cumulative distributions of the number of states where the proportion of extreme  $\text{PM}_{2.5}$  days due to wildfire smoke in a time period met or exceeded a given percentage threshold. For instance, the intersection of a vertical line drawn at 50% and each of the depicted lines in the plot would provide estimates of the number of states in each period where at least 50% of extreme days were due to wildfire smoke.